

MIMO OFDM Radar IRCI Free Range Reconstruction With Sufficient Cyclic Prefix

XIANG-GEN XIA, Fellow, IEEE
University of Delaware
Newark, DE, USA

TIANXIAN ZHANG
LINGJIANG KONG, Senior Member, IEEE
University of Electronic Science and Technology of China
Chengdu Sichuan, P. R. China

In this paper, we propose multiple-input multiple-output (MIMO) orthogonal frequency division multiplexing (OFDM) radar with sufficient cyclic prefix (CP), where all OFDM pulses transmitted from different transmitters share the same frequency band and are orthogonal to each other for every subcarrier in the discrete frequency domain. The orthogonality is not affected by time delays from transmitters. Thus, our proposed MIMO OFDM radar has the same range resolution as single transmitter radar and achieves full spatial diversity. Orthogonal designs are used to achieve this orthogonality across the transmitters, with which it is only needed to design OFDM pulses for the first transmitter. We also propose a joint pulse compression and pulse coherent integration for range reconstruction. In order to achieve the optimal signal-to-noise ratio (SNR) for the range reconstruction, we apply the paraunitary filterbank theory to design the OFDM pulses. We then propose a modified iterative clipping and filtering (MICF) algorithm for the designs of OFDM pulses jointly, when other important factors, such as peak-to-average power ratio (PAPR) in time domain, are also

Manuscript received June 26, 2014; revised November 10, 2014, January 1, 2015; released for publication January 18, 2015.

DOI. No. 10.1109/TAES.2015.140477.

Refereeing of this contribution was handled by F. Gini.

X.-G. Xia's research was partially supported by the Air Force Office of Scientific Research (AFOSR) under Grant FA9550-12-1-0055. T. Zhang's research was supported by the Fundamental Research Funds for the Central Universities under Grant ZYGX2012YB008 and by the China Scholarship Council (CSC) and was done when he was visiting the University of Delaware, Newark, DE. L. Kong's research was supported by the National Natural Science Foundation of China under Grants 61178068, the Fundamental Research Funds of Central Universities under Grants ZYGX2012Z001, the Program for New Century Excellent Talents in University under Grant A1098524023901001063.

Authors' addresses: X.-G. Xia, Department of Electrical and Computer Engineering, University of Delaware, Newark, DE 19716. T. Zhang, L. Kong, School of Electronic Engineering, University of Electronic Science and Technology of China, Chengdu, Sichuan, P.R. China, 611731. E-mail: (tianxian.zhang@gmail.com).

0018-9251/15/\$26.00 © 2015 IEEE

considered. With our proposed MIMO OFDM radar, there is no interference for the range reconstruction not only across the transmitters but also across the range cells in a swath called inter-range-cell interference (IRCI) free that is similar to our previously proposed CP-based OFDM radar for single transmitter. Simulations are presented to illustrate our proposed theory and show that the CP-based MIMO OFDM radar outperforms the existing frequency-band shared MIMO radar with polyphase codes and also frequency division MIMO radar.

I. INTRODUCTION

The multiple-input multiple-output (MIMO) concept using multiple transmit and receive antennas has been intensively investigated in the last decades in wireless communications to collect spatial diversity, see, for example, [1, 2]. In recent years, this concept has been introduced to the radar applications [3–5], which is named “MIMO radar.” Unlike the traditional mono-static radar or phased-array radar, MIMO radar systems employ multiple transmitters, multiple receivers, and multiple orthogonal signals, and can provide more degrees of freedom for the design of a radar system as well as more advantages for radar signal processing. According to the configuration of antennas/transmitters, MIMO radar systems can be divided into two types, namely statistical MIMO radar and colocated MIMO radar. For statistical MIMO radar, the transmitters and receivers are widely separated, then, a target can be observed from different spatial aspects, resulting in spatial diversity and performance improvements of target detection [3], synthetic aperture radar (SAR) applications [6], and direction of arrival estimation [7, 8]. For colocated MIMO radar, the transmitters and receivers are located closely enough. By exploiting waveform diversity, colocated MIMO radar can improve the flexibility for transmit beam design [4, 5], and low-grazing angle target tracking [9].

The above advantages of MIMO radar systems are achieved under the assumption that the transmitted signals are orthogonal to each other in time domain despite their arbitrary time delays. It is well known that this assumption can hold only when the frequency bands of all the transmitted signals do not overlap each other [10]. Then, the signals of different transmitter and receiver pairs can be independently processed and the spatial diversity can be obtained. This MIMO radar system can be denoted as “frequency division MIMO radar” system, which requires a relatively wide frequency band, since each transmitter occupies a unique frequency band. Therefore, the frequency spectrum efficiency is low, especially, for a high range resolution radar system. In other words, the spatial diversity advantage of frequency division MIMO radar systems is built upon the sacrifice of the range resolution. To increase the spectrum efficiency or the range resolution of frequency division MIMO radar systems, there have been many works on investigating “frequency-band shared MIMO radar” systems through the design of time domain orthogonal codes/sequences and/or waveforms, which contain not only good autocorrelation but also good cross-correlation properties [11–18]. However, the design

of binary sequences [11, 12], polyphase sequences [13, 14], unimodular sequence sets [15], or chaotic phase codes [18] can only somewhat mitigate waveform cross-correlation effects or reduce the sidelobes of autocorrelation function. The cross correlations between the delayed time domain waveforms from different transmitters cannot be zero and thus cause interference among transmitters. This limits the collection of the spatial diversity. Therefore, the performance of MIMO radar systems will still be degraded by using the existing designed waveforms.

To deal with the sidelobe issues from the nonideal autocorrelations across the range cells in the conventional SAR systems, in [19, 20] we have proposed a sufficient cyclic prefix (CP) based orthogonal frequency division multiplexing (OFDM) SAR imaging for single transmitter radar systems. By using a sufficient CP, zero range sidelobes and inter-range-cell interference (IRCI) free range reconstruction can be achieved, which provides an opportunity for high resolution range reconstruction. As has been explained in [19], the major differences between our proposed CP-based OFDM SAR and the existing OFDM SAR systems are in two aspects. One is that a sufficiently long CP is used at the transmitter and the CP should be as long as possible when the number of range cells in a swath is large. The other is the SAR imaging algorithm at the receiver, which is not the matched filter receiver by simply treating the CP-based OFDM signals as radar waveforms as is done in the existing OFDM radar systems. With these two differences, the key feature of an OFDM system in communications applications of converting an intersymbol interference (ISI) channel to multiple ISI-free subchannels is analogously obtained in our proposed CP-based OFDM SAR imaging as IRCI free range reconstruction among range cells in a swath.

In this paper, we consider a frequency-band shared statistical MIMO radar range reconstruction using OFDM signals with sufficient CP by generalizing the CP-based OFDM SAR imaging from single transmitter and receiver to multiple transmitter and receiver radar systems called "MIMO OFDM radar." With our newly proposed CP-based MIMO OFDM radar, all the signal waveforms from all the transmitters have the same frequency band and thus the range resolution is not sacrificed and the same as the single transmitter radar. Furthermore, their arbitrarily time delayed versions are still orthogonal for every subcarrier in the discrete frequency domain and therefore, the spatial diversity from all the transmitters can be collected the same as the frequency division MIMO radar. In addition to the two differences mentioned above for single transmitter and receiver CP-based OFDM radar systems with the existing OFDM radar systems, the orthogonality in the time domain under arbitrary time delays between different transmitters has not been considered in most of the existing MIMO OFDM radar systems [6, 8, 9] where IRCI exists not only among range cells in a swath but also among the transmitters. Although it is considered in [7], IRCI is not the focus. In this paper,

IRCI free is achieved among both range cells in a swath and all the transmitters.

We first formulate the problem and describe the MIMO OFDM radar signal model by considering the feature of sufficient CP-based OFDM pulses, where the CP part takes all zero values. Using the properties of frequency domain orthogonal OFDM pulses for every subcarrier between different transmitters, we then derive a MIMO OFDM radar range reconstruction algorithm, which includes the joint processing of pulse compression and pulse coherent integration. We also analyze the change of noise power in every step of the range reconstruction and evaluate the possible signal-to-noise ratio (SNR) degradation caused by the range reconstruction. We then propose the design criterion for the multiple OFDM pulses used at transmitters.

The orthogonality for every subcarrier in the discrete frequency domain among the OFDM waveforms for all the transmitters is done by employing the theory of orthogonal designs [21–28] that has been used as orthogonal space-time codes in MIMO wireless communications [1, 2, 21–28]. To achieve the optimal SNR after the range reconstruction, we propose a joint multiple OFDM pulse design method with a closed-form solution by using paraunitary filterbank theory [29, 30]. With the paraunitary filterbank theory in the design of the MIMO OFDM waveforms, although the SNR after the range reconstruction is maximized, it is not easy to search for the sequences to generate the MIMO OFDM waveforms so that their peak-to-average power ratio (PAPR) is low, while a low PAPR is important in radar practical implementations.

By considering the trade-off between the PAPR and the SNR degradation within the range reconstruction, we propose a modified iterative clipping and filtering (MICF) joint OFDM pulse design method, which can obtain OFDM pulses with low PAPRs and an acceptable SNR degradation. We then present some simulations to demonstrate the performance of the proposed MICF joint OFDM pulse design method. By comparing with the frequency-band shared MIMO radar using polyphase code waveforms and frequency division MIMO radar using linear frequency modulated (LFM) waveforms, we present some simulations to illustrate the performance advantage of the proposed MIMO OFDM radar range reconstruction method. We find that, with the designed OFDM pulses from our proposed MICF method, our proposed CP-based MIMO OFDM radar can obtain the range reconstruction without any interference between different transmitters and achieve the full spatial diversity from all the transmitters and receivers. Meanwhile, it can still maintain the advantage of IRCI free range reconstruction with insignificant SNR degradation and completely avoid the energy redundancy in the case when there are only a limited number of range cells of interest. Note that constant orthogonal/unitary matrices for every subcarrier in the discrete frequency domain across transmitters and waveforms have been constructed in [7] where only a few parameters are used and may limit the waveform designs with other desired properties, such as those discussed above.

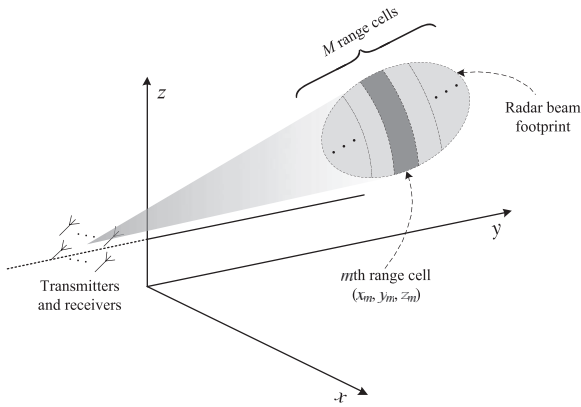


Fig. 1. MIMO OFDM radar geometry.

The remainder of this paper is organized as follows. In Section II, we establish the CP-based MIMO OFDM radar signal model and describe the problem of interest. In Section III, we propose CP-based MIMO OFDM radar range reconstruction. In Section IV, we propose two new arbitrary length OFDM sequence design methods. In Section V, we show some simulation results. Finally, in Section VI, we conclude this paper.

II. CP-BASED MIMO OFDM RADAR SIGNAL MODEL AND PROBLEM FORMULATION

Consider a MIMO radar system with \mathbb{T} transmitters and \mathbb{R} receivers, as shown in Fig. 1. All the antennas of the MIMO radar system we consider in this paper are located in a fixed area, and the antennas are not as close to each other as colocated MIMO radars [4, 5]. The instantaneous coordinate of the α th transmitter and the β th receiver are, respectively, $(x_\alpha, y_\alpha, z_\alpha)$, $\alpha = 1, \dots, \mathbb{T}$, and $(x_\beta, y_\beta, z_\beta)$, $\beta = 1, \dots, \mathbb{R}$, where z_α and z_β are the altitudes of the corresponding antennas. After the demodulation to baseband, the complex envelope of the received signal observed at the β th receiver due to a transmission from the α th transmitter and reflection from the far field scatterers in the m th range cell with instantaneous coordinate (x_m, y_m, z_m) (and excluding noise) is given by

$$u_{\beta,\alpha,m}(t) = g_{\beta,\alpha,m} \exp\{-j2\pi f_c [\tau_{\alpha,m} + \tau_{\beta,m}]\} \times s_\alpha(t - \tau_{\alpha,m} - \tau_{\beta,m}), \quad (1)$$

where $s_\alpha(t)$ is a transmitted signal of the α th transmitter, f_c is the carrier frequency, $g_{\beta,\alpha,m}$ is the radar cross section (RCS) coefficient caused from the scatterers in the m th range cell within the radar mainbeam footprint and related to the α th transmitter and the β th receiver. We assume that the mainbeam footprints of each receiver are overlapped together and included in the footprints of the transmitters. $\tau_{\alpha,m} = \frac{R_{\alpha,m}}{c}$ is the signal propagation time delay between the α th transmitter and the m th range cell, and similarly, $\tau_{\beta,m} = \frac{R_{\beta,m}}{c}$ is the signal propagation time delay between the m th range cell and the β th receiver, where c is the speed of light,

$$R_{\alpha,m} = \sqrt{(x_m - x_\alpha)^2 + (y_m - y_\alpha)^2 + (z_m - z_\alpha)^2} \text{ and}$$

$R_{\beta,m} = \sqrt{(x_m - x_\beta)^2 + (y_m - y_\beta)^2 + (z_m - z_\beta)^2}$ are, respectively, the slant range between the α th transmitter and the m th range cell and the slant range between the m th range cell and the β th receiver.

At the receiver, to a transmitted signal with bandwidth B , the received signal is sampled by the analog-to-digital (A/D) converter with sampling interval length $T_s = \frac{1}{B}$ and the range resolution is $\rho = \frac{c}{2B} = \frac{c}{2} T_s$. Assume that the width for the radar footprints in the range direction is R_w . Then, a range profile can be divided into $M = \frac{R_w}{\rho}$ range cells as in Fig. 1 that is determined by the radar system. From the far field assumption, as we have discussed in [19], we can obtain

$$R_{\alpha,m} = R_{\alpha,0} + m\rho, \quad m = 0, 1, \dots, M-1, \quad (2a)$$

$$R_{\beta,m} = R_{\beta,0} + m\rho, \quad m = 0, 1, \dots, M-1. \quad (2b)$$

Then, the signal propagation time delay between the α th transmitter and the β th receiver can be denoted by

$$\tau_{\alpha,m} + \tau_{\beta,m} = \tau_{\beta,\alpha,0} + mT_s, \quad (3)$$

where

$$\tau_{\beta,\alpha,0} = \frac{R_{\alpha,0} + R_{\beta,0}}{c}. \quad (4)$$

In radar applications, there is usually more than one scatterer within a range cell, and each scatterer owns its unique delay and phase. However, for a given range resolution (or signal bandwidth), a radar is not able to distinguish these individual scatterers, and the responses of all these scatterers are summarized as the response of one range cell with a single delay and phase in the receiver. Thus, each range cell can be treated as one point-like target. This kind of model is reasonable and commonly used in the existing radar applications [31].

Let τ_{min} be the minimal signal propagation time delay between all the transmitter and receiver pairs through the nearest ($m = 0$) range cell. And τ_{min} is defined as

$$\tau_{min} = \min_{\substack{\beta=1,\dots,\mathbb{R} \\ \alpha=1,\dots,\mathbb{T}}} \{\tau_{\beta,\alpha,0}\}. \quad (5)$$

By arranging the antennas, the time delays between different transmitter and receiver pairs can approximately satisfy the relationship

$$\eta_{\beta,\alpha} = \frac{\tau_{\beta,\alpha,0} - \tau_{min}}{T_s}, \quad (6)$$

where $\eta_{\beta,\alpha} \in \mathbb{N}$. The maximal relative time delay difference among all the transmitter and receiver pairs is $\eta_{max} T_s$, and

$$\eta_{max} = \max_{\beta,\alpha} \{\eta_{\beta,\alpha}\}. \quad (7)$$

We remark that the values of $\eta_{\beta,\alpha}$ may slightly change, when a radar scans the radar surveillance area with different azimuth angle. But, in practice, considering the far field assumption, $\eta_{\beta,\alpha}$ is constant within a consecutive

radar scan sector. Thus, the radar surveillance area can be divided into different radar scan sectors with different precalculated values of $\eta_{\beta,\alpha}$. Also, parameter η_{max} is determined by the system configuration and may be estimated a priori, and it is used for the MIMO OFDM pulse designs later.

In most of the MIMO radar literature, it is assumed that the transmitted signals are orthogonal to each other and even when there are different time delays among these signals, i.e., $\int s_\alpha(t)s_{\tilde{\alpha}}(t-\tau)^*dt = 0$ for $\alpha \neq \tilde{\alpha}$, and arbitrary time delay c of interest, where $(\cdot)^*$ denotes the complex conjugate, or it is assumed that there are no different time delays among the transmitted signals from multiple transmitters. However, in practice, this is generally not possible [10], unless the frequency bands of all the transmitted signals do not overlap with each other, which then leads to frequency division MIMO radar and will either reduce the range resolution or not be able to collect the transmitter spatial diversity as we have mentioned in the Introduction. As we see later in this paper, these two assumptions will not be needed with our proposed MIMO OFDM radar.

In this paper, we consider that there are P coherent pulses in a radar coherent processing interval (CPI) (as we see later that some of these P pulses may be all zero-valued). Each non-zero-valued pulse is an OFDM signal with N subcarriers and a bandwidth of B Hz. Let $\mathbf{S}_\alpha^{(p)} = [S_{\alpha,0}^{(p)}, S_{\alpha,1}^{(p)}, \dots, S_{\alpha,N-1}^{(p)}]^T$ represent the complex weights transmitted over the subcarriers of the p th OFDM pulse and the α th transmitter, where $p = 0, 1, \dots, P-1$, and $(\cdot)^T$ denotes the transpose. For convenience, we normalize the total transmitted energy within a CPI to 1, and assume the energy of each transmitted pulse is the same, i.e., $\sum_{k=0}^{N-1} |S_{\alpha,k}^{(p)}|^2 = \frac{1}{P_1}$ for all non-zero-valued pulses where P_1 is the number of non-zero-valued pulses. All the transmitted signals share the same frequency band. Then, a discrete time OFDM signal is the inverse fast Fourier transform (IFFT) of the vector $\mathbf{S}_\alpha^{(p)}$ and the corresponding time domain OFDM signal is

$$s_\alpha^{(p)}(t) = \frac{1}{\sqrt{N}} \sum_{k=0}^{N-1} S_{\alpha,k}^{(p)} \exp\{j2\pi k \Delta f t\}, \quad (8)$$

$$t \in [pT_r, pT_r + T + T_{GI}],$$

where $\Delta f = \frac{B}{N} = \frac{1}{T}$ is the subcarrier spacing, and T_r is the time interval between two consecutive pulses within a CPI. $[pT_r, pT_r + T_{GI}]$ is the time duration of the guard interval that corresponds to the CP in the discrete time domain as we see later in more detail and its length T_{GI} is specified later as well; T is the length of the OFDM signal excluding CP. Due to the periodicity of the exponential function $\exp(\cdot)$ in (8), the tail part of $s_\alpha^{(p)}(t)$ for t in $[pT_r, pT_r + T + T_{GI}]$ is the same as the head part of $s_\alpha^{(p)}(t)$ for t in $[pT_r, pT_r + T_{GI}]$. Note that in the above transmission, the CP is added to each pulse $s_\alpha^{(p)}(t)$.

Then, the complex envelope of the received signal in the β th receiver due to the p th transmitted pulses of all the transmitters and the reflection from all range cells within the mainbeam footprint can be written as

$$u_\beta^{(p)}(t) = \frac{1}{\sqrt{N}} \sum_{\alpha=1}^{\mathbb{T}} \sum_{m=1}^{M-1} g_{\beta,\alpha,m} \exp\{-j2\pi f_c [\tau_{\alpha,m} + \tau_{\beta,m}]\} \times \sum_{k=0}^{N-1} S_{\alpha,k}^{(p)} \exp\left\{\frac{j2\pi k}{T} [t - \tau_{\alpha,m} - \tau_{\beta,m}]\right\} + w_\beta^{(p)}(t), \quad (9)$$

where $w_\beta^{(p)}(t)$ represents the noise. For convenience, in this paper, we assume the RCS coefficients $g_{\beta,\alpha,m}$ are constant within a CPI, and it can be generalized to the case of maneuvering targets similar to what is done in the literature.

In our MIMO radar applications, the values of time delays $\tau_{\beta,\alpha,0}$ are different from one transmitter and receiver pair to another, which depend on the relative locations of antennas. All the received signals due to \mathbb{T} transmitters and reflections from each range cell will overlap together at the receiver and cannot be separated in general. Thus, the interferences will occur including different range cells and different transmitted signals from the transmitters and result in IRCI. Notice that, to one range cell, each transmitter and receiver pair can be regarded as one path of communications, and, to one transmitter and receiver pair each range cell can also be regarded as one path of communications as analyzed in [19]. Comparing with the main path that we define as the shortest path, the longest time delay among all the paths is $(\eta_{max} + M - 1)T_s$. As we have mentioned in [19], to eliminate the interference between different transmitted signals and IRCI, similar to OFDM systems in communications, the time duration of guard interval should be at least $(\eta_{max} + M - 1)T_s$. For convenience, we use CP length $\eta_{max} + M - 1$ in this paper, i.e., a CP of length $\eta_{max} + M - 1$ is added at the beginning of an OFDM pulse, and then the guard interval length T_{GI} in the analog transmission signal is $T_{GI} = (\eta_{max} + M - 1)T_s$. Notice that $T = NT_s$, so the time duration of an OFDM pulse is $T_o = T + T_{GI} = (N + \eta_{max} + M - 1)T_s$. To completely avoid the range interference between different transmitted signals and range cells, the number N of the OFDM signal subcarriers should satisfy $N \geq \eta_{max} + M$ as we have analyzed in [19] and will be seen in more detail later, and it is also well understood in communications applications [32].

III. CP-BASED MIMO OFDM RADAR RANGE RECONSTRUCTION

This section is on the MIMO radar range reconstruction that includes the joint processing of pulse compression and pulse coherent integration. Going back to (9), for the p th pulse, let the sampling at all receivers be

aligned with the start of the received signals after $pT_r + \tau_{min}$ seconds of the transmitted pulses, where we recall that T_r is the time interval between two consecutive pulses. Combining with (3), (6), and (9), $u_\beta^{(p)}(t)$ can be converted to the discrete time linear convolution of the transmitted sequence with the weighting RCS coefficients $d_{\beta,\alpha,m}$ after the sampling $t = pT_r + \tau_{min} + iT_s$ and the received sequence can be written as

$$\tilde{u}_{\beta,i}^{(p)} = \sum_{\alpha=1}^{\mathbb{T}} \sum_{m=0}^{M-1} d_{\beta,\alpha,m} s_{\alpha,i-m-\eta_{\beta,\alpha}}^{(p)} + \tilde{w}_{\beta,i}^{(p)},$$

$$i = 0, 1, \dots, N + 2(\eta_{max} + M) - 3, \quad (10)$$

where

$$d_{\beta,\alpha,m} = g_{\beta,\alpha,m} \exp\{-j2\pi f_c[\tau_{\alpha,m} + \tau_{\beta,m}]\}, \quad (11)$$

in which $2\pi f_c[\tau_{\alpha,m} + \tau_{\beta,m}]$ in the exponential is known and related to the target location,¹ and $s_{\alpha,i}^{(p)}$ is the complex envelope of the OFDM pulse in (8) with time duration $t \in [pT_r, pT_r + T + T_{GI}]$ for $T = NT_s$ and $T_{GI} = (\eta_{max} + M - 1)T_s$. In (10), $\tilde{w}_{\beta,i}^{(p)}$ is the noise. After sampling at $t = pT_r + iT_s$, (8) can be recast as

$$s_{\alpha,i}^{(p)} = s_\alpha^{(p)}(iT_s) = \frac{1}{\sqrt{N}} \sum_{k=0}^{N-1} S_{\alpha,k}^{(p)} \exp\left\{\frac{j2\pi ki}{N}\right\},$$

$$i = 0, 1, \dots, N + \eta_{max} + M - 2, \quad (12)$$

and $s_{\alpha,i}^{(p)} = 0$ if $i < 0$ or $i > N + \eta_{max} + M - 2$.

When the sequence

$\tilde{\mathbf{u}}_\beta = [\tilde{u}_{\beta,0}, \tilde{u}_{\beta,1}, \dots, \tilde{u}_{\beta,N+2(\eta_{max}+M)-3}]^T$ in (10) is received, the first and the last $\eta_{max} + M - 1$ samples are removed as [19], and then, we obtain

$$u_{\beta,n}^{(p)} = \sum_{\alpha=1}^{\mathbb{T}} \sum_{m=0}^{M-1} d_{\beta,\alpha,m} s_{\alpha,n+\eta_{max}+M-m-\eta_{\beta,\alpha}-1}^{(p)} + w_{\beta,n}^{(p)},$$

$$n = 0, 1, \dots, N - 1. \quad (13)$$

The OFDM demodulator then performs the N -point fast Fourier transform (FFT) on the vector

$\mathbf{u}_\beta^{(p)} = [u_{\beta,0}^{(p)}, \dots, u_{\beta,N-1}^{(p)}]^T$, and obtains $\mathbf{U}_\beta^{(p)} = [U_{\beta,0}^{(p)}, \dots, U_{\beta,N-1}^{(p)}]^T$, where $U_{\beta,k}^{(p)}$ can be denoted as

$$U_{\beta,k}^{(p)} = \mathbf{D}_{\beta,k} \bar{\mathbf{S}}_k^{(p)} + W_{\beta,k}^{(p)}, \quad k = 0, 1, \dots, N - 1, \quad (14)$$

where $\bar{\mathbf{S}}_k^{(p)} = [S_{1,k}^{(p)}, \dots, S_{\mathbb{T},k}^{(p)}]^T$ is a $\mathbb{T} \times 1$ column vector.

$W_{\beta,k}^{(p)}$ is the FFT of noise, and $\mathbf{D}_{\beta,k} = [D_{\beta,1,k}, \dots, D_{\beta,\mathbb{T},k}]$ with

$$D_{\beta,\alpha,k} = \sum_{m=0}^{M-1} d_{\beta,\alpha,m} \exp\left\{\frac{j2\pi k(\eta_{max} + M - \eta_{\beta,\alpha} - 1)}{N}\right\}$$

$$\times \exp\left\{\frac{-j2\pi km}{N}\right\}, \quad k = 0, 1, \dots, N - 1, \quad (15)$$

¹ Notice that the values of $j2\pi f_c \tau_{\alpha,m}$ and $j2\pi f_c \tau_{\beta,m}$ form the transmitter steering vector and receiver steering vector [33], respectively, which are often assumed known.

where, $d_{\beta,\alpha,m}$ is the weighting RCS coefficient from the α th transmitter, the m th range cell, and the β th receiver.

From the constant assumption of $g_{\beta,\alpha,m}$ within a CPI, for given β , α , and m , the values of $d_{\beta,\alpha,m}$ in (11) and $D_{\beta,\alpha,k}$ in (15) are also constant within a CPI. Combining all the received signals of \mathbb{R} receivers and P pulses within a CPI, we can obtain the following matrix representation:

$$\mathbf{U}_k = \mathbf{D}_k \mathbf{S}_k + \mathbf{W}_k, \quad k = 0, 1, \dots, N - 1, \quad (16)$$

where $\mathbf{U}_k = [\mathbf{U}_k^{(0)}, \mathbf{U}_k^{(1)}, \dots, \mathbf{U}_k^{(P-1)}]$ is an $\mathbb{R} \times P$ matrix, $\mathbf{U}_k^{(p)} = [U_{1,k}^{(p)}, U_{2,k}^{(p)}, \dots, U_{\mathbb{R},k}^{(p)}]^T$ is an $\mathbb{R} \times 1$ column vector for $0 \leq p \leq P - 1$.

$$\mathbf{S}_k \triangleq [\bar{\mathbf{S}}_k^{(0)}, \bar{\mathbf{S}}_k^{(1)}, \dots, \bar{\mathbf{S}}_k^{(P-1)}] = \begin{bmatrix} S_{1,k}^{(0)} & S_{1,k}^{(1)} & \dots & S_{1,k}^{(P-1)} \\ S_{2,k}^{(0)} & S_{2,k}^{(1)} & \dots & S_{2,k}^{(P-1)} \\ \vdots & \vdots & \ddots & \vdots \\ S_{\mathbb{T},k}^{(0)} & S_{\mathbb{T},k}^{(1)} & \dots & S_{\mathbb{T},k}^{(P-1)} \end{bmatrix} \quad (17)$$

is a $\mathbb{T} \times P$ matrix. $\mathbf{W}_k = [\mathbf{W}_k^{(0)}, \mathbf{W}_k^{(1)}, \dots, \mathbf{W}_k^{(P-1)}]$ is an $\mathbb{R} \times P$ matrix, $\mathbf{W}_k^{(p)} = [W_{1,k}^{(p)}, W_{2,k}^{(p)}, \dots, W_{\mathbb{R},k}^{(p)}]^T$ is an $\mathbb{R} \times 1$ column vector. And

$$\mathbf{D}_k = \begin{bmatrix} D_{1,1,k} & D_{1,2,k} & \dots & D_{1,\mathbb{T},k} \\ D_{2,1,k} & D_{2,2,k} & \dots & D_{2,\mathbb{T},k} \\ \vdots & \vdots & \ddots & \vdots \\ D_{\mathbb{R},1,k} & D_{\mathbb{R},2,k} & \dots & D_{\mathbb{R},\mathbb{T},k} \end{bmatrix} \quad (18)$$

is an $\mathbb{R} \times \mathbb{T}$ matrix.

By assuming $P \geq \mathbb{T}$, we can construct such a $\mathbb{T} \times P$ matrix \mathbf{S}_k to guarantee $\mathbf{S}_k \mathbf{S}_k^+ = \mathbf{I}_{\mathbb{T}}$ for all k , where $\mathbf{I}_{\mathbb{T}}$ is the $\mathbb{T} \times \mathbb{T}$ identity matrix, $\mathbf{S}_k^+ = \mathbf{S}_k^\dagger (\mathbf{S}_k \mathbf{S}_k^\dagger)^{-1} \in \mathbb{C}^{P \times \mathbb{T}}$ is the Penrose-Moore pseudoinverse of \mathbf{S}_k , and $(\cdot)^\dagger$ denotes the conjugate transpose. Note that as long as matrix \mathbf{S}_k has full row rank, i.e., $1 \times P$ weight vectors in the P OFDM waveforms from all transmitters are linearly independent on every subcarrier k , property $\mathbf{S}_k \mathbf{S}_k^+ = \mathbf{I}_{\mathbb{T}}$ is satisfied.

Then, the estimate of \mathbf{D}_k in (16) is

$$\hat{\mathbf{D}}_k = \mathbf{U}_k \mathbf{S}_k^+ = \mathbf{D}_k + \bar{\mathbf{W}}_k, \quad (19)$$

where $\bar{\mathbf{W}}_k = \mathbf{W}_k \mathbf{S}_k^+$ denotes the new noise matrix. One can see from the above estimate that the new noise matrix is obtained by multiplying the inverse of matrix \mathbf{S}_k to the original noise matrix \mathbf{W}_k for each subcarrier index k . Clearly, in order not to enhance the noise, it is desired that the matrix \mathbf{S}_k is unitary, which is similar to the MIMO OFDM channel estimation in wireless communications [1, 2, 32]. Since \mathbf{S}_k is a flat matrix in general, in what follows we require that the row vectors of \mathbf{S}_k are orthogonal to each other and have the same norm called flat unitary matrix, i.e., $\mathbf{S}_k \mathbf{S}_k^\dagger = \mathbf{I}_{\mathbb{T}}$. This means that the weight vectors at every subcarrier k in the OFDM waveforms transmitted through \mathbb{T} transmitters are orthogonal to each other among different transmitters, i.e., the discrete versions in frequency domain are orthogonal to each other for every subcarrier, which still holds when there are time delays

among the corresponding waveforms in time domain, although the delayed waveforms may not be orthogonal in time domain. This property is fundamentally different from most of the existing MIMO radars including the existing MIMO OFDM radars.

According to (15), vector $\mathbf{D}_{\beta,\alpha} = [D_{\beta,\alpha,0}, D_{\beta,\alpha,1}, \dots, D_{\beta,\alpha,N-1}]^T$ is just the N -point FFT of vector $\sqrt{N}\gamma$, where γ is an N -dimensional vector, which is a right cyclic shift of $\eta_{max} + M - \eta_{\beta,\alpha} - 1$ positions of vector

$$\left[d_{\beta,\alpha,0}, d_{\beta,\alpha,1}, \dots, d_{\beta,\alpha,M-1}, \underbrace{0, \dots, 0}_{N-M} \right]^T,$$

where $d_{\beta,\alpha,m}$ are the weighting RCS coefficients, similar to the single transmitter and single receiver case studied in [19].

Then, the pulse compression and coherent integration can be achieved by performing the N -point IFFT operation on vector $\hat{\mathbf{D}}_{\beta,\alpha} = [\hat{D}_{\beta,\alpha,0}, \hat{D}_{\beta,\alpha,1}, \dots, \hat{D}_{\beta,\alpha,N-1}]^T$ and we obtain

$$\tilde{d}_{\beta,\alpha,\tilde{m}} = \frac{1}{\sqrt{N}} \sum_{n=0}^{N-1} \hat{D}_{\beta,\alpha,n} \exp \left\{ \frac{j2\pi \tilde{m} n}{N} \right\},$$

$$\tilde{m} = 0, 1, \dots, N-1. \quad (20)$$

So, the estimate of $d_{\beta,\alpha,m}$ can be achieved by a left cyclic shift of $\eta_{max} + M - \eta_{\beta,\alpha} - 1$ positions of vector $\tilde{d}_{\beta,\alpha,\tilde{m}}$, i.e., vector $[\hat{d}_{\beta,\alpha,0}, \dots, \hat{d}_{\beta,\alpha,M-1}]^T$ is equal to the first M elements of vector

$$[\tilde{d}_{\beta,\alpha,N-\eta_{max}-M+\eta_{\beta,\alpha}+1}, \dots, \tilde{d}_{\beta,\alpha,N-1}, \tilde{d}_{\beta,\alpha,0}, \dots, \tilde{d}_{\beta,\alpha,N-\eta_{max}-M+\eta_{\beta,\alpha}}]^T.$$

We then obtain the following estimates of the M weighting RCS coefficients at the β th receiver due to the α th transmitter:

$$\hat{d}_{\beta,\alpha,m} = \sqrt{N} d_{\beta,\alpha,m} + w_{\beta,\alpha,m}, \quad m = 0, 1, \dots, M-1, \quad (21)$$

where $w_{\beta,\alpha,m}$ is the m th output of the N -point IFFT of the vector $[\bar{W}_{\beta,\alpha,0}, \bar{W}_{\beta,\alpha,1}, \dots, \bar{W}_{\beta,\alpha,N-1}]^T$ that is the β th row and the α th column element of matrix $\bar{\mathbf{W}}_k$ for $k = 0, 1, \dots, N-1$. $\bar{W}_{\beta,\alpha,k}$ can be written as

$$\bar{W}_{\beta,\alpha,k} = \frac{\sum_{p=0}^{P-1} W_{\beta,k}^{(p)} S_{\alpha,k}^{(p)}}{\sum_{p=0}^{P-1} |S_{\alpha,k}^{(p)}|^2}, \quad k = 0, 1, \dots, N-1. \quad (22)$$

In (21), $d_{\beta,\alpha,m}$ can be recovered without any interference from other transmitted signals or IRCI from other range cells. Then, using (11), we can compensate the phase and obtain the estimate of the RCS coefficient $g_{\beta,\alpha,m}$ as

$$\hat{g}_{\beta,\alpha,m} = \hat{d}_{\beta,\alpha,m} \exp \{ j2\pi f_c [\tau_{\alpha,m} + \tau_{\beta,m}] \}. \quad (23)$$

In the above joint pulse compression and coherent integration, the operations of FFT in (14), the estimate of \mathbf{D}_k in (19), and IFFT in (20) are applied. Thus, we need to

analyze the changes of the noise power in each step of the above range reconstruction method. Assume that the noise component $w_{\beta,n}^{(p)}$ in (13) is a complex white Gaussian variable with zero-mean and the same variance σ^2 , i.e., $w_{\beta,n}^{(p)} \sim \mathcal{CN}(0, \sigma^2)$ for all receivers β , pulses p , and samples n . Since the FFT operation is unitary, after the process in (14), the additive noise power of $W_{\beta,k}^{(p)}$ does not change, i.e., $W_{\beta,k}^{(p)} \sim \mathcal{CN}(0, \sigma^2)$. In the same way, the noise power of each element in \mathbf{W}_k in (16) is also σ^2 . However, after the operation for the estimate of \mathbf{D}_k in (19), the variance of a noise component $\bar{W}_{\beta,\alpha,k}$ in (22) can be calculated as

$$E \{ \bar{W}_{\beta,\alpha,k} \bar{W}_{\beta,\alpha,k}^\dagger \} = \sigma^2 \left[\sum_{p=0}^{P-1} |S_{\alpha,k}^{(p)}|^2 \right]^{-1},$$

and thus

$$\bar{W}_{\beta,\alpha,k} \sim \mathcal{CN} \left(0, \sigma^2 \left[\sum_{p=0}^{P-1} |S_{\alpha,k}^{(p)}|^2 \right]^{-1} \right),$$

$$k = 0, 1, \dots, N-1,$$

for all β and α . Moreover, after the IFFT operation in (20), we then have finished the joint pulse compression and coherent integration. The noise power of $w_{\beta,\alpha,m}$ in (21) is

$$E \{ w_{\beta,\alpha,m} w_{\beta,\alpha,m}^\dagger \} = \frac{\sigma^2}{N} \sum_{k=0}^{N-1} \left[\sum_{p=0}^{P-1} |S_{\alpha,k}^{(p)}|^2 \right]^{-1}$$

and

$$w_{\beta,\alpha,m} \sim \mathcal{CN} \left(0, \frac{\sigma^2}{N} \sum_{k=0}^{N-1} \left[\sum_{p=0}^{P-1} |S_{\alpha,k}^{(p)}|^2 \right]^{-1} \right).$$

Thus, from (21), we can obtain the SNR of the signal after the joint pulse compression and coherent integration at the β th receiver due to the transmission from the α th transmitter and reflected from the m th range cell as,

$$\text{SNR}_{\beta,\alpha,m} = \frac{N^2 |d_{\beta,\alpha,m}|^2}{\sigma^2 \sum_{k=0}^{N-1} \left[\sum_{p=0}^{P-1} |S_{\alpha,k}^{(p)}|^2 \right]^{-1}}. \quad (24)$$

Notice that a larger $\text{SNR}_{\beta,\alpha,m}$ can be obtained with a smaller value of

$$\sum_{k=0}^{N-1} \left[\sum_{p=0}^{P-1} |S_{\alpha,k}^{(p)}|^2 \right]^{-1}$$

by designing $S_{\alpha,k}^{(p)}$. With a given α th transmitter and the energy constraint

$$\sum_{p=0}^{P-1} \sum_{k=0}^{N-1} |S_{\alpha,k}^{(p)}|^2 = \frac{1}{\mathbb{T}},$$

when $\sum_{p=0}^{P-1} |S_{\alpha,k}^{(p)}|^2$ has constant module for all k , i.e.,

$$\sum_{p=0}^{P-1} |S_{\alpha,0}^{(p)}|^2 = \sum_{p=0}^{P-1} |S_{\alpha,1}^{(p)}|^2 = \dots = \sum_{p=0}^{P-1} |S_{\alpha,N-1}^{(p)}|^2 = \frac{1}{N\mathbb{T}}, \quad (25)$$

we obtain the minimal value of

$$\sum_{k=0}^{N-1} \left[\sum_{p=0}^{P-1} |S_{\alpha,k}^{(p)}|^2 \right]^{-1} = N^2\mathbb{T}.$$

In this case, the maximal SNR after the joint pulse compression and coherent integration can be obtained as

$$\text{SNR}_{\beta,\alpha,m}^{(\max)} = \max_{\tilde{\mathbf{S}}_\alpha, \|\tilde{\mathbf{S}}_\alpha\|^2 = \frac{1}{\mathbb{T}}} \{ \text{SNR}_{\beta,\alpha,m} \} = \frac{|d_{\beta,\alpha,m}|^2}{\mathbb{T}\sigma^2}, \quad (26)$$

where $\tilde{\mathbf{S}}_\alpha = \left[(S_\alpha^{(0)})^T, \dots, (S_\alpha^{(P-1)})^T \right]^T \in \mathbb{C}^{PN \times 1}$.

Thus, for the α th transmitter, the optimal signal $S_{\alpha,k}^{(p)}$ should satisfy a requirement that the transmitted energy summations of the P pulses within a CPI, i.e., $\sum_{p=0}^{P-1} |S_{\alpha,k}^{(p)}|^2$, have constant module for all k . Otherwise, the SNR after the range reconstruction will be degraded. Here, we define the SNR degradation factor as

$$\xi = \frac{\text{SNR}_{\beta,\alpha,m}}{\text{SNR}_{\beta,\alpha,m}^{(\max)}} = \frac{N^2\mathbb{T}}{\sum_{k=0}^{N-1} \left[\sum_{p=0}^{P-1} |S_{\alpha,k}^{(p)}|^2 \right]^{-1}}. \quad (27)$$

Notice that $\xi \in (0,1]$ is independent of the noise power σ^2 and the weighting RCS coefficient $d_{\beta,\alpha,m}$. Since we assume that the row vectors of matrix \mathbf{S}_k are orthogonal to each other and have the same norm, the above degradation factor ξ is also independent of β and α . The SNR degradation factor ξ in (27) is for the performance of both pulse compression and coherent integration of all the P pulses within a CPI, but not only the pulse compression of a single pulse in [20].

We recall that the number of the OFDM signal subcarriers should satisfy $N \geq \eta_{\max} + M$. Thus, the length of the transmitted signals should be increased with the increases of the width R_w for the radar footprints in the range direction and/or η_{\max} . The pulse length will be much longer than the traditional radar pulse for a wide width R_w (or large M) and/or a large delay η_{\max} , which may be a problem, especially for covert/military radar applications. Meanwhile, the CP removal for the elimination of the interference at the receivers may cause high transmitted energy redundancy as we have mentioned in [20].

Therefore, it is necessary for us to achieve MIMO OFDM radar with arbitrary pulse length that is independent of R_w . The main idea is to generate P pulses

$s_\alpha^{(p)}(t)$, $t \in [pT_r, pT_r + T + T_{GI}]$, $p = 0, 1, \dots, P-1$, for all \mathbb{T} transmitters, such that the discrete time sequence of $s_\alpha^{(p)}(t)$, $pT_r \leq t \leq pT_r + T + T_{GI}$:

$s_{\alpha,i}^{(p)} = s_\alpha^{(p)}(iT_s)$, $0 \leq i \leq N + \eta_{\max} + M - 2$ in (12), is zero at the head and the tail parts as

$$\begin{aligned} \left[s_{\alpha,0}^{(p)}, \dots, s_{\alpha,\eta_{\max}+M-2}^{(p)} \right]^T &= \left[s_{\alpha,N}^{(p)}, \dots, s_{\alpha,N+\eta_{\max}+M-2}^{(p)} \right]^T \\ &= \mathbf{0}_{(\eta_{\max}+M-1) \times 1}. \end{aligned} \quad (28)$$

In the meantime, $s_{\alpha,i}^{(p)}$ is also a sampled discrete time sequence of an OFDM pulse in (8) for $t \in [pT_r, pT_r + T + T_{GI}]$. This zero head and tail condition (28) is the same as that in [20]. Then, in this case, the continuous time signal $s_\alpha^{(p)}(t)$ is only transmitted on the time interval $t \in [pT_r + T_{GI}, pT_r + T]$ that has length $T - T_{GI}$, where T_{GI} is the length of the guard interval and also the zero-valued head part of the signal that leads to the zero-valued CP part at the tail. Since T can be arbitrarily designed, the OFDM pulse length $T - T_{GI}$ can be arbitrary as well. For more details, we refer to [20]. Based on the above analysis, the key task of the following section is the design of these multiple OFDM sequences.

IV. DESIGN OF MULTIPLE OFDM SEQUENCES

In this section, we design the weight sequences in the P OFDM pulses for each transmitter, i.e., the matrix $\mathbf{S}_k = [S_{\alpha,k}^{(p)}]_{1 \leq \alpha \leq \mathbb{T}, 0 \leq p \leq P-1}$ for $k = 0, 1, \dots, N-1$ in (17). There are three indices here: one is the transmitter index α , one is the OFDM pulse index p for each transmitter, and the third one is the subcarrier index k . We start with the design criterion.

A. Design Criterion

Any segment of an OFDM pulse in (8) is determined by a weight sequence $\mathbf{S}_\alpha^{(p)} = [S_{\alpha,0}^{(p)}, S_{\alpha,1}^{(p)}, \dots, S_{\alpha,N-1}^{(p)}]^T$ that is determined by its N -point IFFT $s_\alpha^{(p)} = [s_{\alpha,0}^{(p)}, s_{\alpha,1}^{(p)}, \dots, s_{\alpha,N-1}^{(p)}]^T$. Thus, the design of $s_\alpha^{(p)}$ is equivalent to the design of $\mathbf{S}_\alpha^{(p)}$. Based on the above discussions, $s_\alpha^{(p)}$ and $\mathbf{S}_\alpha^{(p)}$ should satisfy the following conditions.

1) *Frequency domain orthogonality among transmitters for every subcarrier:* As was mentioned earlier, in order not to enhance the noise in the estimate in (19) for RCS coefficients, matrix \mathbf{S}_k has to be a flat unitary matrix, i.e., $\mathbf{S}_k \mathbf{S}_k^\dagger = \mathbf{I}_\mathbb{T}$ for each $k = 0, 1, \dots, N-1$. Specifically, the sequence $\mathbf{S}_{\alpha,k}$ should be orthogonal to sequence $\mathbf{S}_{\tilde{\alpha},k}$ for different transmitters $\alpha \neq \tilde{\alpha}$ and $1 \leq \alpha, \tilde{\alpha} \leq \mathbb{T}$, and have the same norm, where $\mathbf{S}_{\alpha,k} = [S_{\alpha,k}^{(0)}, S_{\alpha,k}^{(1)}, \dots, S_{\alpha,k}^{(P-1)}]$ is the α th row of \mathbf{S}_k . Note that this orthogonality is for every subcarrier in the discrete frequency domain of the signal waveforms but not in the time domain as commonly used in a MIMO radar. The advantage of this orthogonality in the frequency domain is that it is not affected by time delays in the time domain, while the orthogonality in the time domain is sensitive to any time delays. In addition, this discrete orthogonality in the frequency domain does not require that the frequency bands of the waveforms do not overlap each other as commonly used in the frequency division MIMO radar

and in fact, all the frequency bands of the \mathbb{T} waveforms can be the same. It implies that the range resolution is not sacrificed as is done in frequency division MIMO radar. This criterion deals with the transmitter index α and the OFDM pulse index p , and the subcarrier index k is free.

2) *Zero head and tail condition:* Sequence $s_\alpha^{(p)}$ should satisfy the zero head and tail condition in (28) for all p and α . This criterion only deals with the time index i in a pulse, or equivalently, the subcarrier index k .

3) *Flat total spectral power of P pulses:* To avoid the SNR degradation as the estimation of the weighting RCS coefficients in (19) and what follows, and achieve the maximal SNR after pulse compression and coherent integration, for the α th transmitter, the transmitted energy summation of all the P pulses within a CPI should have constant module for all k , i.e.,

$$\sum_{p=0}^{P-1} |S_{\alpha,k}^{(p)}|^2 = \frac{1}{N\mathbb{T}}.$$

This criterion only deals with the pulse index p .

4) *Good PAPR property:* The PAPR of the transmitted OFDM pulse $s_\alpha^{(p)}(t)$, $p = 0, 1, \dots, P - 1$, in (8) for $t \in [pT_r + T_{GI}, pT_r + T]$ should be minimized for an easy practical implementation of the radar. This criterion also only deals with the time index t in a pulse, or equivalently, the subcarrier index k .

The basic idea of the following designs to satisfy the above four criteria is to first use a pattern (called orthogonal design) of placing P pulses to ensure the orthogonality condition 1) among all the \mathbb{T} transmitters, where the P pulses and/or their complex conjugates and/or their shifted versions etc. are used by every transmitter. After this is done, it is only needed to work on these P pulses to satisfy the other three criteria above, which are independent of a transmitter.

B. Frequency Domain Orthogonality Using Orthogonal Designs

The orthogonality condition 1) for the weighting matrix \mathbf{S}_k in (17) is for all subcarrier indices k , i.e., it is for a matrix whose entries are variables but not simply constants. This motivates us to use complex orthogonal designs (COD) [21–28] whose entries are arbitrary complex variables. Furthermore, each row vector of a COD uses the same set of complex variables, which corresponds to each transmitter using the same set of OFDM pulses and therefore we only need to consider P pulses for one transmitter as explained above.

Let us briefly recall a COD [21–28]. A $\mathbb{T} \times P$ COD² with P_1 complex variables x_1, x_2, \dots, x_{P_1} is a $\mathbb{T} \times P$

² The COD definition we use in this paper follows the original COD definition [22, 26] where no linear combinations or repetitions of complex variables x_i is allowed in the matrix entry or any row of the matrix. This appears important in the applications in this paper. More general COD definitions can be found in [22, 25, 26, 28] where any complex linear combinations of complex variables x_i are allowed in the

matrix \mathbf{X} such that its every entry is either 0, x_i , $-x_i$, x_i^* , or $-x_i^*$ and satisfies the following identity

$$\mathbf{X}\mathbf{X}^\dagger = (|x_1|^2 + \dots + |x_{P_1}|^2) \mathbf{I}_{\mathbb{T}}, \quad (29)$$

where every x_i may take any complex value. CODs have been used for orthogonal space-time block codes (OSTBC) in MIMO communications to collect full spatial diversity with fast maximum likelihood (ML) decoding, see for example [21–28]. Note that, as we see later, our use of a COD in the following is not from an OSTBC point of view but only from the structured orthogonality (29). A closed-form inductive design of a $\mathbb{T} \times P$ COD for any \mathbb{T} is given in [28]. The following are two simple but nontrivial COD for $\mathbb{T} = 2$ and 4, respectively,

$$\mathbf{X}_2 = \begin{bmatrix} x_1 & x_2 \\ -x_2^* & x_1^* \end{bmatrix} \text{ and } \mathbf{X}_4 = \begin{bmatrix} x_1 & x_2 & x_3 & 0 \\ -x_2^* & x_1^* & 0 & x_3 \\ -x_3^* & 0 & x_1^* & -x_2 \\ 0 & -x_3^* & x_2^* & x_1 \end{bmatrix}. \quad (30)$$

The above COD \mathbf{X}_2 was first used as an OSTBC by Alamouti in [21] and it is now well known as Alamouti code in MIMO communications. From the second example \mathbf{X}_4 above, one may see that the number P_1 of the nonzero variables in a COD may not be necessarily equal to the number P of its columns. In fact, for a given \mathbb{T} , the relationship between P , P_1 , and \mathbb{T} has been given in [26, 28], where it is shown that

$$\frac{P_1}{P} = \frac{\lceil \frac{\mathbb{T}}{2} \rceil + 1}{2 \lceil \frac{\mathbb{T}}{2} \rceil} \quad (31)$$

is achieved with closed-form designs in [28]. From the COD definition, it is not hard to see that every row of a COD contains the same set of complex variables x_1, \dots, x_{P_1} and every such variable x_i only appears once. With this property, when we apply a COD as a weighting matrix \mathbf{S}_k for every k , among the P pulses, only P_1 nonzero OFDM pulses are used for every transmitter and the other $P - P_1$ pulses are all zero-valued.

With a COD, we may design a weighting matrix \mathbf{S}_k for every k . Let us use the above 2×2 COD as an example. It is used for the case of $\mathbb{T} = P = 2$. The corresponding 2×2 weighting matrix \mathbf{S}_k for every k is

$$\begin{bmatrix} \mathbf{S}_{1,k} \\ \mathbf{S}_{2,k} \end{bmatrix} = \begin{bmatrix} S_{1,k}^{(0)} & S_{1,k}^{(1)} \\ S_{2,k}^{(0)} & S_{2,k}^{(1)} \end{bmatrix} = \begin{bmatrix} S_{1,k}^{(0)} & S_{1,k}^{(1)} \\ -(S_{1,k}^{(1)})^* & (S_{1,k}^{(0)})^* \end{bmatrix}, \quad k = 0, 1, \dots, N - 1. \quad (32)$$

Then, $\mathbf{S}_{1,k}$ and $\mathbf{S}_{2,k}$ are orthogonal and have the same norm for every k . The discrete time domain sequences $s_\alpha^{(p)} = [s_{\alpha,0}^{(p)}, \dots, s_{\alpha,N-1}^{(p)}]^T$ for the α th transmitter and the p th OFDM pulse is obtained by taking the N -point IFFT of $\mathbf{S}_\alpha^{(p)} = [S_{\alpha,0}^{(p)}, \dots, S_{\alpha,N-1}^{(p)}]^T$. From the above design in (32)

entries of the matrix and does not affect their applications in wireless MIMO communications.

for two transmitters, the two OFDM pulses for the first transmitter are free to design so far, while the two OFDM pulses for the second transmitter in the frequency domain are determined by the two pulses for the first transmitter. The two OFDM pulses for the second transmitter in the discrete time domain are, correspondingly,

$$s_{2,i}^{(0)} = -\left(s_{1,N-i}^{(1)}\right)^* \text{ and } s_{2,i}^{(1)} = \left(s_{1,N-i}^{(0)}\right)^*, \quad i=0, 1, \dots, N-1.$$

In the continuous time domain, they are

$$s_2^{(0)}(t) = -\left(s_1^{(1)}(T-t)\right)^* \text{ and } s_2^{(1)}(t) = \left(s_1^{(0)}(T-t)\right)^*,$$

where $t \in [T_{GI}, T + T_{GI}]$ when the CP is not included and $t \in [0, T + T_{GI}]$ when the CP is included.

For general \mathbb{T} transmitters, from a COD design [28], such as (30) for $\mathbb{T} = 4$, the discrete complex weight sequences for the first transmitter $\mathbf{S}_1^{(p)} = [S_{1,0}^{(p)}, \dots, S_{1,N-1}^{(p)}]^T$ are either the all zero sequence ($P - P_1$ of them) or free to design (P_1 of them) so far (more conditions will be imposed for the other criteria, 2)–4), later). The discrete complex weight sequences for any other transmitter $\mathbf{S}_\alpha^{(p)} = [S_{\alpha,0}^{(p)}, \dots, S_{\alpha,N-1}^{(p)}]^T$ for $\alpha > 1$ are either the all zero sequence ($P - P_1$ of them as the first transmitter), or $\pm \mathbf{S}_1^{(p')}$, or $\pm (\mathbf{S}_1^{(p')})^*$ for some p' with $0 \leq p' \neq p \leq P - 1$. Then, the discrete time domain sequences for any other transmitter $s_{\alpha,i}^{(p)}$ for $\alpha > 1$ are either the all zero sequence or $\pm [s_{1,i}^{(p')}]_{0 \leq i \leq N-1}$ or $\pm ([s_{1,N-i}^{(p')}]_{0 \leq i \leq N-1})^*$ for some p' with $0 \leq p' \neq p \leq P - 1$. In the continuous time domain, a pulse transmitted by any other transmitter $s_\alpha^{(p)}(t)$ for $\alpha > 1$ are either the all zero-valued pulse, or $\pm s_1^{(p')}(t)$ or $\pm (s_1^{(p')}(T-t))^*$ for some p' with $0 \leq p' \neq p \leq P - 1$. Note that for notational convenience, all the above P pulses are considered over the same time interval. However, these P pulses are arranged sequentially in time after they are designed and when they are used/transmitted.

In the case of $\mathbb{T} = 4$ in (30), $P_1 = 3$ and $P = 4$ and there is one all zero pulse for each transmitter and at any time, only three transmitters transmit signals and the idle transmitter alternates.

From the above pulse placement among transmitters using a COD, the transmitted pulses for the first transmitter are either all zero-valued, or free to design, and the pulses transmitted by any other transmitters are the pulses transmitted by the first transmitter possibly with some simple operations of negative signed, complex conjugated, and/or time-reversed in the pulse period, and no more and no less pulses are transmitted. These operations do not change the signal power in frequency domain or the signal PAPR in time domain for a pulse, and thus do not change the conditions 3) and 4) of the design criteria studied above. So, for the design criteria 3) and 4), we only need to consider the P_1 nonzero pulses for the first transmitter. Note that the complex conjugation in frequency domain not only causes the complex conjugation in time domain but also causes the time reversal in time domain as

expressed above. The time reversal operation to a pulse in time domain may change the zero head and tail condition 2) in the above design criteria, i.e., if a sequence satisfies the zero head and tail condition (28), its time-reversed version may not satisfy the zero head and tail condition (28) anymore. However, if sequence $s_\alpha^{(p)}$, with its FFT $\mathbf{S}_\alpha^{(p)}$, satisfies not only the condition in (28) but also

$$\left[s_{\alpha,N-\eta_{max}-M+2}^{(p)}, \dots, s_{\alpha,N-1}^{(p)} \right]^T = \mathbf{0}_{(\eta_{max}+M-2) \times 1}, \quad (33)$$

then, not only sequence $s_\alpha^{(p)} = [s_{\alpha,i}^{(p)}]$ satisfies the zero head and tail condition (28) but also its time-reversed version $[s_{\alpha,N-i}^{(p)}]$ also satisfies the zero head and tail condition (28). Due to this additional zero-segment condition in (33), the PAPR in time domain should be redefined as the PAPR only over the nonzero portion, i.e., the portion for $t \in [pT_r + T_{GI}, pT_r + T - T_{GI} + T_s]$, of a pulse. Therefore, the design criteria 2) and 4) should be updated as follows.

2) *New zero head and tail condition:* Sequence $s_\alpha^{(p)}$ should satisfy the zero head and tail conditions in (28) and (33) for all p and α .

4) *New good PAPR property:* The PAPR of the transmitted non-zero-valued OFDM pulse $s_\alpha^{(p)}(t)$ for each $p, p = 0, 1, \dots, P_1 - 1$, and each $\alpha, 1 \leq \alpha \leq \mathbb{T}$, in (8) for $t \in [pT_r + T_{GI}, pT_r + T - T_{GI} + T_s]$ should be minimized.

In this case, with the conditions in (28) and (33), a transmitted time domain sequence of the α th transmitter and the p th pulse becomes $\tilde{s}_\alpha^{(p)} = [s_{\alpha,\eta_{max}+M-1}^{(p)}, s_{\alpha,\eta_{max}+M}^{(p)}, \dots, s_{\alpha,N-\eta_{max}-M+1}^{(p)}]^T \in \mathbb{C}^{N_t \times 1}$ for $1 \leq \alpha \leq \mathbb{T}$ and $0 \leq p \leq P - 1$, where $N_t = N - 2\eta_{max} - 2M + 3$ is the length of the transmitted nonzero OFDM sequences. Among these P pulses, only P_1 of them are not all zero pulses. Thus, the normalized transmitted energy constraint of $\tilde{s}_\alpha^{(p)}$ is that the mean transmitted power of $\tilde{s}_\alpha^{(p)}$ is $\frac{1}{N_t \mathbb{T} P_1}$. Hence, the SNR of the received signal from the m th range cell before pulse compression and coherent integration is

$$\overline{\text{SNR}}_{\beta,\alpha,m} = \frac{|d_{\beta,\alpha,m}|^2}{N_t \mathbb{T} P_1 \sigma^2}. \quad (34)$$

Note that the maximal SNR of the m th range cell after the joint pulse compression and coherent integration $\text{SNR}_{\beta,\alpha,m}^{(max)}$ in (26) is equal to $P_1 N_t \overline{\text{SNR}}_{\beta,\alpha,m}$, and the SNR gains of the pulse coherent integration P_1 (the number of nonzero pulses) and the pulse compression N_t (the non-zero-valued pulse length) are consistent with the traditional radar applications [31]. Based on the above analysis, the key task of the remainder of this section is to design a sequence $s_\alpha^{(p)}$ that simultaneously satisfies the above criteria 2), 3), and 4).

Before finishing this subsection, a remark on using a COD in the above pulse placement among transmitters is made as follows. When the number \mathbb{T} of transmitters is not small, either the number P of pulses will be much larger than \mathbb{T} or the number P_1 of nonzero pulses can be put in will be small. There is a trade-off among these three parameters as we have mentioned earlier for a COD

design. When P_1 is small, there are less degrees of freedom in the pulse design, which will affect the MIMO OFDM radar performance, when other conditions are imposed as we see later. Furthermore, when P_1 is small, the radar transmitter usage is low and may not be preferred in radar applications. From the COD rate property (31), one can see that P_1 is always more than $P/2$, i.e., among a CPI of P pulses, there are always more than half of P pulses that are nonzero OFDM pulses. A trivial unitary matrix \mathbf{S}_k in (17) is a diagonal matrix with all diagonal elements of the same norm. This corresponds to the case when there is only one transmitter that transmits at any time in a CPI and then the radar transmitter usage becomes the lowest, which is again not preferred. On the other hand, when P is large, the time to transmit these P pulses becomes long, which may not be preferred in some radar applications either. Another remark is that unitary matrices \mathbf{S}_k have been also constructed in [7] where all unitary matrices \mathbf{S}_k for all k are from a single constant unitary matrix and each \mathbf{S}_k for each k has only one free parameter on phase. This may limit the ability to find desired waveforms with some additional desired properties, such as those we discuss next.

Also in what follows, for the notational convenience, we use P instead of P_1 to denote the number of nonzero OFDM pulses to design since an all-zero-valued pulse does not affect the other pulses.

C. Flat Total Spectral Power Using Paraunitary Filterbanks

From the above studies, we only need to design P pulses for the first transmitter. In this subsection, we design P OFDM pulses by designing their equivalent OFDM sequences $s^{(p)}$ in time domain or $S^{(p)}$ in frequency domain, for $p = 0, 1, \dots, P-1$, that satisfy the design criteria 2) (new) and 3) precisely. We omit their transmitter index 1 for convenience. The main idea is to apply the paraunitary filterbank theory [29] ([30] for a short tutorial) as follows.

Considering the above criterion 2) (new), the complex weight sequences $S^{(p)}$, for $p = 0, 1, \dots, P-1$, can be written as

$$S_k^{(p)} = \frac{1}{\sqrt{N}} \sum_{i=\eta_{1st}}^{N-\eta_{1st}} s_i^{(p)} \exp\left\{-\frac{j2\pi ik}{N}\right\}, \quad k=0, 1, \dots, N-1, \quad (35)$$

where $\eta_{1st} = \eta_{max} + M - 1$ is the index of the first nonzero value of sequence $s^{(p)}$. Then, we have $S_k^{(p)} = S^{(p)}(z)|_{z=W_k}$ for $k = 0, 1, \dots, N-1$, where $W_k \triangleq \exp\{j\frac{2\pi k}{N}\}$ and

$$S^{(p)}(z) = \frac{z^{-\eta_{1st}}}{\sqrt{N}} \sum_{i=0}^{N_i-1} s_{\eta_{1st}+i}^{(p)} z^{-i}, \quad (36)$$

where we recall that $N_i = N - 2\eta_{max} - 2M + 3$ is the length of the transmitted nonzero OFDM sequences. Then, the flat total spectral power in the criterion 3) can be

rewritten as

$$\sum_{p=0}^{P-1} \left| S^{(p)}(z) \right|_{z=W_k}^2 = \frac{1}{N\mathbb{T}}, \quad k = 0, 1, \dots, N-1. \quad (37)$$

The above identity for all k is ensured by the following identity on the whole unit circle of z ,

$$\sum_{p=0}^{P-1} |S^{(p)}(z)|^2 = \frac{1}{N\mathbb{T}}, \quad |z| = 1. \quad (38)$$

This identity tells us that if $S^{(p)}(z)$, $p = 0, 1, \dots, P-1$, form a filterbank, then this filterbank can be systematically constructed by a paraunitary filterbank with polyphase representations of P filters $S^{(p)}(z)$, $p = 0, 1, \dots, P-1$ [29] as follows. For each p , rewrite $S^{(p)}(z)$ as

$$S^{(p)}(z) = z^{-\eta_{1st}} \sum_{q=0}^{P-1} z^{-q} S_q^{(p)}(z^P), \quad (39)$$

where

$$S_q^{(p)}(z) = \frac{1}{\sqrt{N}} \sum_{i=0}^{\lfloor \frac{N_i-p}{P} \rfloor} s_{\eta_{1st}+Pi+q}^{(p)} z^{-i} \quad (40)$$

is the q th polyphase component of $S^{(p)}(z)$. Clearly, a filter $S^{(p)}(z)$ and its P polyphase components $S_q^{(p)}(z)$, $q = 0, 1, \dots, P-1$, can be equivalently and easily converted to each other as above. These P^2 polyphase components for all the P filters form a $P \times P$ polyphase matrix $\mathbf{S}(z) = [S_q^{(p)}(z)]_{0 \leq p \leq P-1, 0 \leq q \leq P-1}$. Then, the flat spectral power condition (38) is equivalent to the losslessness (or paraunitariness) of the $P \times P$ matrix $\mathbf{S}(z)\tilde{\mathbf{S}}(z) = \frac{1}{N\mathbb{T}}\mathbf{I}_P$ for all complex values $|z| = 1$ (or all complex values z and then this matrix is called a paraunitary matrix) [29], where $\tilde{\mathbf{S}}(z)$ is the tilde operation of $\mathbf{S}(z)$, i.e., $\tilde{\mathbf{S}}(z) = \mathbf{S}^\dagger(z^{-1})$. Such a paraunitary matrix can be factorized as [29]

$$\mathbf{S}(z) = \frac{1}{\sqrt{N\mathbb{T}}} \prod_{l=1}^{\lfloor \frac{N_i-p}{P} \rfloor} \mathbf{V}_l(z)\mathbf{V}, \quad (41)$$

where \mathbf{V} is a $P \times P$ constant unitary matrix and

$$\mathbf{V}_l(z) = \mathbf{I}_P - v_l v_l^\dagger + z^{-1} v_l v_l^\dagger, \quad (42)$$

where $\mathbf{v}_l \in \mathbb{C}^{P \times 1}$ is a P by 1 constant column vector of unit norm.

In order to construct OFDM sequences $s^{(p)}$ that satisfy the new zero head and tail condition 2), when $\frac{N_i-p}{P}$ is not an integer, the above paraunitary matrix $\mathbf{S}(z)$ can be constructed as

$$\mathbf{S}(z) = \frac{1}{\sqrt{N\mathbb{T}}} \prod_{l=1}^{\lfloor \frac{N_i-p}{P} \rfloor} \mathbf{V}_l(z)\mathbf{V}, \quad (43)$$

where \mathbf{V} and $\mathbf{V}_l(z)$ are as in (41) and (42), respectively.

After a paraunitary matrix $\mathbf{S}(z) = [S_q^{(p)}(z)]$ is constructed

in (43), we can form $S^{(p)}(z)$ for $p = 0, 1, \dots, P-1$ via (39). Then, sequences $S_k^{(p)}$, $k = 0, 1, \dots, N-1$, for $p = 0, 1, \dots, P-1$, satisfy the flat total spectral power condition 3). The discrete time domain OFDM sequences $s^{(p)}$ can be obtained by taking the N -point IFFT of $S^{(p)}$ for every $p = 0, 1, \dots, P-1$, which satisfy the new zero head and tail condition 2). In this construction, there are P^2 complex-valued parameters in the unitary matrix V and $\lfloor \frac{N_t - P}{P} \rfloor \times P$ complex-valued parameters in the $P \times 1$ vectors v_l with unit norm for $l = 1, 2, \dots, \lfloor \frac{N_t - P}{P} \rfloor$. Therefore, there are total

$$P^2 + \left\lfloor \frac{N_t - P}{P} \right\rfloor \times P \approx N_t + P^2 - P$$

complex-valued parameters to choose under the constraints of $VV^T = I_P$ and $\|v_l\| = 1$. As a remark, compared with the single OFDM pulse case studied for single transmitter radar in [19, 20] i.e., $P = 1$, the flat total spectral power 3) for $P > 1$ is easier to achieve.

In order to design OFDM pulses to satisfy the criterion 4), i.e., to have low PAPR in the time domain, unfortunately, there is no closed-form construction (see, for example, a tutorial [35] for PAPR issues) as for the previous three criteria 1)–3). One way to design good PAPR pulses satisfying 1)–3) is to search the above parameters in V and v_l . However, since there are too many complex-valued parameters to search, it is hard to find OFDM pulses that satisfy 1)–3) and have good PAPR property in time domain. Let us go back to reexam the flat total spectral power property 3) that is used to achieve the optimal SNR after the joint pulse compression and coherent integration as is studied in (24)–(26). In practice, a small SNR degradation with $\xi \approx 1$ in (27) may not impact the radar performance much by slightly relaxing the flat total spectral power condition 3). With this small relaxation, i.e., $\sum_{p=0}^{P-1} |S_k^{(p)}|^2 \approx \frac{1}{N_T}$ for all $k = 0, 1, \dots, N-1$, it will be much easier to achieve good PAPR criterion 4) as we see below.

D. OFDM Sequence Design Using MICF

A simple method was proposed in [20] for single OFDM pulse design, in which the filtering and clipping operations were iteratively applied in time and frequency domains to reduce the PAPR of the transmitted OFDM pulse and make the complex weights of different subcarriers to be as constant as possible. Since the above requirements 2), 3), and 4) are respectively similar³ to the corresponding requirements 1), 2), and 3) in [20], by using the method in [20], a simple method to achieve $\sum_{p=0}^{P-1} |S_k^{(p)}|^2 \approx \frac{1}{N_T}$ and the zero head and tail condition 2) is to design each individual sequence $S_k^{(p)}$ for each p

³ The difference is that an additional condition of (33) is added in the above requirement 3 of this paper.

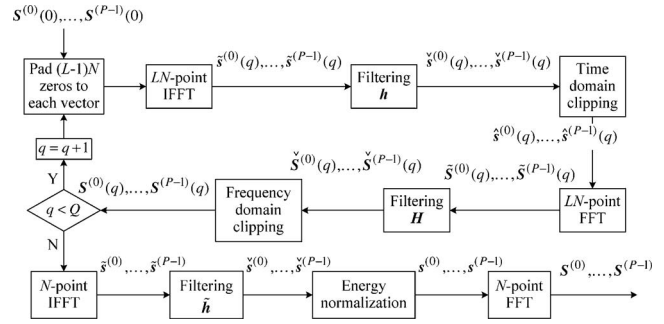


Fig. 2. Block diagram of joint multiple OFDM sequence design using MICF.

separately for approximately constant module $S_k^{(p)}$ for all k and p , i.e., $|S_k^{(p)}| \approx \frac{1}{\sqrt{N_T P}}$. However, with this simple method, there are less degrees of freedom than that when all P pulses are jointly considered in the design, which can be evidenced by observing that there are closed-form solutions to achieve the flat total spectral power when $P > 1$ as studied in the preceding subsection, while it is much harder (if not impossible) when $P = 1$. In the meantime, there are more degrees of freedom for filtering and clipping when all P OFDM pulses are designed jointly and then, the above requirements 2)–4) can be better satisfied. Therefore, in the following, we propose an MICF algorithm to design P OFDM pulses jointly.

For convenience to deal with the PAPR issue, our proposed MICF algorithm starts with some initial random constant modular sequences $S^{(p)}(0) \in \mathbb{C}^{N \times 1}$, for $p = 0, 1, \dots, P-1$. Then, at the q th iteration, $(L-1)N$ zeros are padded to each sequence $S^{(p)}(q)$ as $[S_0^{(p)}(q), \dots, S_{N-1}^{(p)}(q), \mathbf{0}_{1 \times (L-1)N}]^T$ and we obtain $\tilde{s}^{(p)}(q) \in \mathbb{C}^{LN \times 1}$ by using LN -point IFFT, as shown in the block diagram Fig. 2, where $\tilde{s}^{(p)}$ denote the time domain OFDM sequences by L times oversampling of the continuous waveforms $s^{(p)}(t)$. Since the first $\eta_{max} + M - 1$ and the last $\eta_{max} + M - 2$ samples of our desired sequences $s^{(p)}$ should be equal to zero, we apply the following time domain filter to the sequences $\tilde{s}^{(p)}(q)$:

$$h(n) = \begin{cases} 0, & 0 \leq n \leq L(\eta_{max} + M - 1) - 1 \\ 1, & L(\eta_{max} + M - 1) \leq n \leq L(N - \eta_{max} - M + 2) - 1, \\ 0, & L(N - \eta_{max} - M + 2) \leq n \leq LN - 1 \end{cases} \quad (44)$$

to obtain new sequences $\check{s}^{(p)}(q) = [\check{s}_0^{(p)}(q), \dots, \check{s}_{LN-1}^{(p)}(q)]^T$, where $\check{s}_n^{(p)}(q) = \tilde{s}_n^{(p)}(q)h(n)$, $n = 0, 1, \dots, LN - 1$. The time domain clipping [20] is then applied to the segment of the nonzero elements of the sequence $\check{s}^{(p)}(q)$ with a preset constant lower bound $PAPR_d$ as a desired PAPR, and we obtain the sequence $\hat{s}^{(p)}(q)$. After the LN -point FFT and frequency domain filtering, we obtain the sequences $\tilde{S}^{(p)}(q)$ and $\check{S}^{(p)}(q)$, respectively. Notice that the frequency domain filtering is used to constrain the out-of-band radiation caused by the time domain filtering

and clipping. To deal with the constant transmitted energy among N subcarriers of the summation for all the P pulses, the following frequency domain clipping is used:

$$S_k^{(p)}(q+1) = \begin{cases} \sqrt{\frac{\text{Pav}(q)(1+G_f)}{P_k(q)}} \tilde{S}_k^{(p)}(q), & \text{if } P_k(q) > \text{Pav}(q)(1+G_f) \\ \sqrt{\frac{\text{Pav}(q)(1-G_f)}{P_k(q)}} \tilde{S}_k^{(p)}(q), & \text{if } P_k(q) < \text{Pav}(q)(1-G_f), \\ \tilde{S}_k^{(p)}(q), & \text{otherwise} \end{cases} \quad (45)$$

where $0 < k < N-1$, we obtain $\mathbf{S}^{(p)}(q+1) = [S_0^{(p)}(q+1), S_1^{(p)}(q+1), \dots, S_{N-1}^{(p)}(q+1)]^T$, and

$$P_k(q) = \sum_{p=0}^{P-1} \left| \tilde{S}_k^{(p)}(q) \right|^2$$

and

$$\text{Pav}(q) = \frac{1}{N} \sum_{k=0}^{N-1} P_k(q)$$

are, respectively, the transmitted energy of the k th subcarrier of the summation for all the P pulses and the average energy of N subcarriers for all the P pulses within a CPI. G_f is a factor that we use to control the upper and

lower bounds for $\sum_{p=0}^{P-1} |S_k^{(p)}(q+1)|^2$. Thus, the value of

$\sum_{p=0}^{P-1} |S_k^{(p)}(q+1)|^2$ is constrained as $\sum_{p=0}^{P-1} |S_k^{(p)}(q+1)|^2 \in [\text{Pav}(q)(1-G_f), \text{Pav}(q)(1+G_f)]$. A smaller G_f

denotes that a closer-to-constant value $\sum_{p=0}^{P-1} |S_k^{(p)}(q+1)|^2$ can be obtained.

In Fig. 2, Q is a preset maximum iteration number. When $q = Q$, the iteration stops and the N -point IFFT will be applied to the sequence $\mathbf{S}^{(p)}(Q) \in \mathbb{C}^{N \times 1}$ to obtain $\tilde{\mathbf{s}}^{(p)} \in \mathbb{C}^{N \times 1}$. Then, a time domain filter,

$$\tilde{h}(n) = \begin{cases} 0, & 0 \leq n \leq \eta_{\max} + M - 2 \\ 1, & \eta_{\max} + M - 1 \leq n \leq N - \eta_{\max} - M + 1 \\ 0, & N - \eta_{\max} - M + 2 \leq n \leq N - 1 \end{cases},$$

is applied to $\tilde{\mathbf{s}}^{(p)}$ and we obtain sequence $\check{\mathbf{s}}^{(p)} = [\check{s}_0^{(p)}, \dots, \check{s}_{N-1}^{(p)}]^T$, where $\check{s}_n^{(p)} = \tilde{s}_n^{(p)} \tilde{h}(n)$, for $n = 0, 1, \dots, N-1$. To normalize the transmitted energy and

make sure $\sum_{k=0}^{N-1} |S_k^{(p)}|^2 = \frac{1}{\mathbb{T}P}$ for each pulse, the

normalization is applied to the sequence $\check{\mathbf{s}}^{(p)}$, i.e.,

$$s_n^{(p)} = \frac{\check{s}_n^{(p)}}{\sqrt{\mathbb{T}P \sum_{i=\eta_{\max}+M-1}^{N-\eta_{\max}-M+1} |\check{s}_i^{(p)}|^2}}, \quad n = 0, 1, \dots, N-1,$$

and we obtain OFDM sequence $\mathbf{s}^{(p)}$ that accurately satisfies the new zero head and tail criterion 2). Finally,

sequence $\mathbf{S}^{(p)}$ can be obtained by using the N -point FFT to $\mathbf{s}^{(p)}$. The PAPR of the nonzero part of $\mathbf{s}^{(p)}$ can be obtained from $\mathbf{S}^{(p)}$ [20]. The SNR degradation factor ξ in (27) can also be calculated from $\mathbf{S}^{(p)}$, $p = 0, 1, \dots, P-1$.

A remark to finish this section is that in radar applications our proposed MIMO OFDM pulse design can be done off-line and as long as one set of P_1 nonzero OFDM pulses are found with the above desired properties, it is good enough and the convergence of the above proposed iterative algorithm is not very important.

V. SIMULATION RESULTS

In this section, we first study the performance of our proposed MICF OFDM sequence/pulse design by using Monte Carlo simulations. We then study the performance of the MIMO OFDM radar detection with our designed OFDM pulses. From what was studied in the preceding section, P_1 nonzero OFDM pulses need to be designed.

A. Performance of the MICF OFDM Pulse Design

In this subsection, we first see the performance of the MICF OFDM pulse design algorithm. We set the number of range cells $M = 96$, the maximum relative time delays $\eta_{\max} = 40$, the number of subcarriers $N = 302$, and the nonzero pulse length $N_t = 33$. To achieve a sufficiently accurate PAPR estimate, we set the oversampling ratio $L = 4$ [34, 35]. We evaluate the mean PAPR of the P pulses and the SNR degradation factor ξ by using the standard Monte Carlo technique with 2000 independent trials. In each trial, the k th element of an initial sequence $\mathbf{S}_a^{(p)}(0)$ is set as $S_{a,k}^{(p)}(0) = \frac{1}{\sqrt{N\mathbb{T}P}} e^{j2\pi\phi_k^{(p)}}$, $k = 0, 1, \dots, N-1$, where $\phi_k^{(p)}$ is uniformly distributed within the interval $[0, 2\pi]$. In Figs. 3–5, we plot the cumulative distribution functions (cdf) of the mean PAPR and the SNR degradation factor ξ with $P = 4$. The curves in Fig. 3 denote that, with the increase of the maximum iteration number Q , the mean PAPR decreases and ξ increases. Therefore, better P OFDM pulses with lower mean PAPR and larger ξ can be obtained by using a larger iteration number Q . The curves in Fig. 4 show that, with the increase of PAPR_d , the mean PAPR increases and ξ decreases; in the meantime the mean PAPR change is more sensitive than the change of ξ for different PAPR_d . Similarly, the curves in Fig. 5 indicate that the mean PAPR is decreased and the SNR degradation is increased, when G_f is increased. In summary, the simulation results of mean PAPR and ξ are better than the corresponding results for single OFDM pulse design (corresponding to the case of $P = 1$) in [20] even though with a small value of Q as shown in Fig. 6, which is because the joint design of P OFDM pulses provides more degrees of freedom for the MICF algorithm. We also plot the cdfs of mean PAPR and ξ for different pulse numbers P with $Q = 8$, $\text{PAPR}_d = 0.1$ dB, and $G_f = 10\%$ in Fig. 6. The curves in Fig. 6 show that, with the increase of P , the mean PAPR and ξ are significantly improved, where one can see that the single OFDM pulse design, i.e., when $P =$

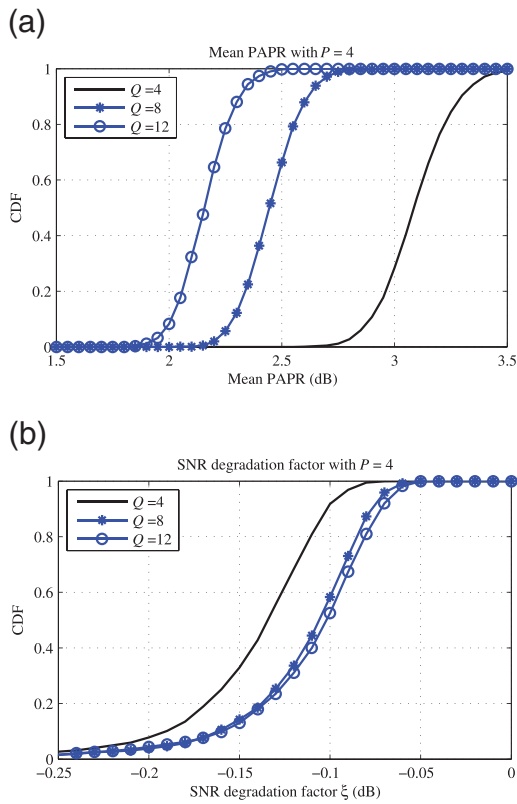


Fig. 3. CDFs for different Q with $P = 4$, $\text{PAPR}_d = 0.1$ dB, and $G_f = 10\%$. (a) Mean PAPR. (b) SNR degradation factor.

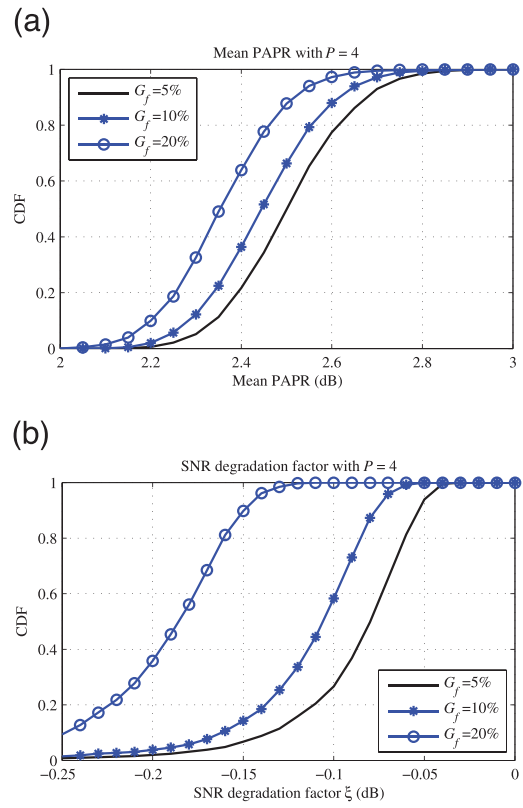


Fig. 5. CDFs for different G_f with $P = 4$, $Q = 8$, and $\text{PAPR}_d = 0.1$ dB. (a) Mean PAPR. (b) SNR degradation factor.

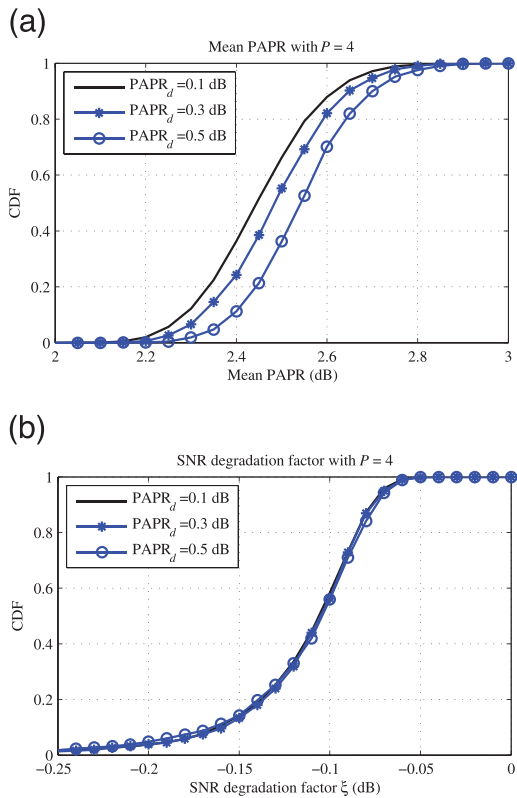


Fig. 4. CDFs for different PAPR_d with $P = 4$, $Q = 8$, and $G_f = 10\%$. (a) Mean PAPR. (b) SNR degradation factor.

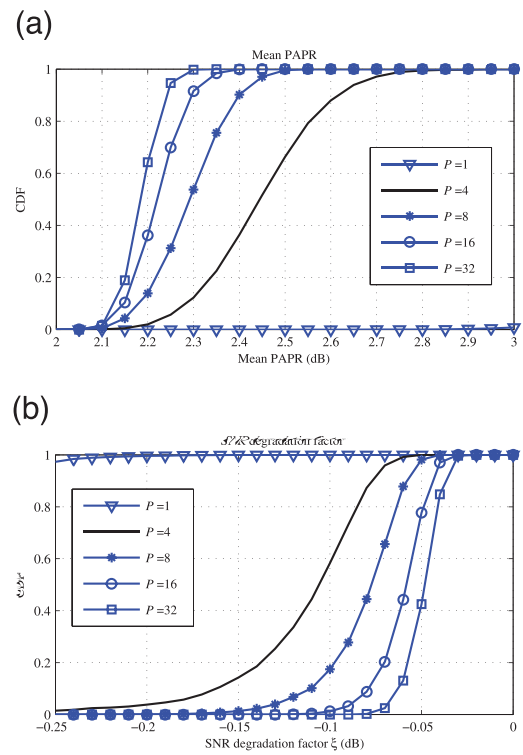


Fig. 6. CDFs for different P with $Q = 8$, $\text{PAPR}_d = 0.1$ dB, and $G_f = 10\%$. (a) Mean PAPR. (b) SNR degradation factor.

TABLE I

Numbers of Monte Carlo Trials for $\xi \geq -0.08$ dB and Mean PAPR ≤ 2.2 dB with $Q = 8$, $\text{PAPR}_d = 0.1$ dB, and $G_f = 10\%$

$P = 4$	$P = 8$	$P = 16$	$P = 32$
14	169	680	1282
Total number of trials: 2000			

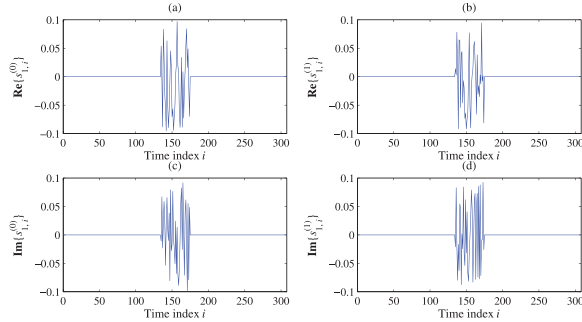


Fig. 7. Our designed OFDM pulses for transmitter $\alpha = 1$. (a) Real part of transmitted pulse $s_1^{(0)}$; (b) Real part of transmitted pulse $s_1^{(1)}$; (c) Imaginary part of transmitted pulse $s_1^{(0)}$; (d) Imaginary part of transmitted pulse $s_1^{(1)}$.

1, is poor because the small iteration number $Q = 8$ is used. It further indicates the benefits of the proposed MICF algorithm with joint design of P OFDM pulses.

According to the above analysis, the mean PAPR and ξ are interacting with each other. In practice, it is necessary to consider the constraints of both mean PAPR and ξ at the same time. In Table I, we count the numbers of trials under the conditions of $\xi \geq -0.08$ dB and mean PAPR ≤ 2.2 dB within the 2000 Monte Carlo independent trials for $Q = 8$, $\text{PAPR}_d = 0.1$ dB, and $G_f = 10\%$. The numbers of trials are increased significantly with the increase of P . According to our simulations, there are 7 trials that satisfy the conditions of $\xi \geq -0.04$ dB and mean PAPR ≤ 2.1 dB with $P = 32$, which are not shown in Table I.

B. Performance of the MIMO OFDM Radar Range Reconstruction

In this subsection, we investigate the performance of the MIMO OFDM radar range reconstruction. We set the bandwidth $B = 150$ MHz, the carrier frequency $f_c = 9$ GHz, the number of range cells $M = 96$, the maximum relative time delay $\eta_{max} = 40$, the number of subcarriers $N = 309$, the length of a nonzero pulse $N_t = 40$, the number of transmitters $\mathbb{T} = 2$ and the number of receivers $\mathbb{R} = 2$, the number of pulses $P = 2$. We use our designed OFDM pulses with the degradation factor $\xi = -0.07$ dB and mean PAPR = 2.06 dB. Our designed OFDM pulses are shown in Fig. 7. For convenience, the time delays $\eta_{\beta,\alpha}$ are randomly chosen within the integer interval $[0, \eta_{max}]$ as $\eta_{1,1} = 17, \eta_{1,2} = 0, \eta_{2,1} = 6, \eta_{2,2} = 32$. Considering a single range line, the targets (nonzero RCS coefficients) are included in 10 random range cells located from 10 000 m to 10 096 m. The RCS coefficients $g_{\beta,\alpha,m}$ within the 10 range cells are independent and obey complex white

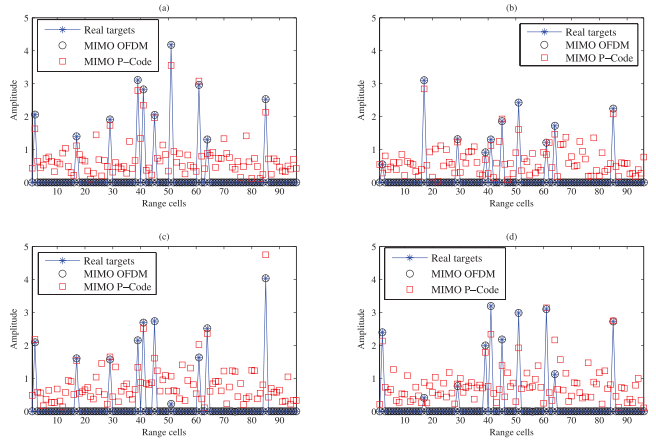


Fig. 8. Amplitudes of targets for different transmitter and receiver pairs after range reconstructions without noise using polyphase waveforms and our designed OFDM pulses with transmitter and receiver pair. (a) $(\alpha, \beta) = (1, 1)$. (b) $(\alpha, \beta) = (2, 1)$. (c) $(\alpha, \beta) = (1, 2)$. (d) $(\alpha, \beta) = (2, 2)$.

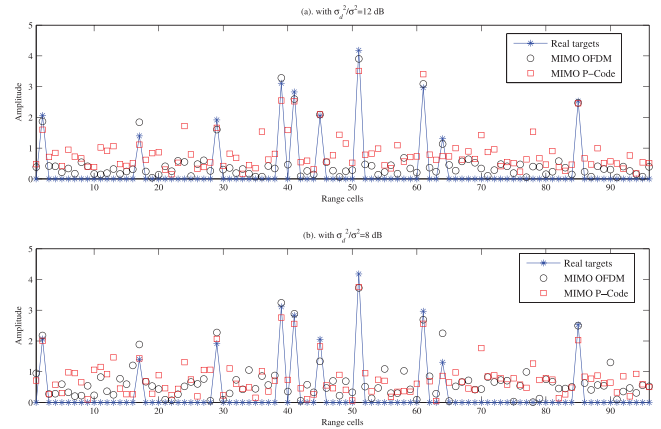


Fig. 9. Amplitudes of targets for $(\alpha, \beta) = (1, 1)$ after range reconstructions using polyphase waveforms and our designed OFDM pulses. (a) With $\frac{\sigma_d^2}{\sigma_s^2} = 12$ dB. (b) With $\frac{\sigma_d^2}{\sigma_s^2} = 8$ dB.

Gaussian distribution with zero-mean and variance σ_d^2 , i.e., $g_{\beta,a,m} \sim \mathcal{CN}(0, \sigma_d^2)$ for all receivers β and transmitters α . For comparison, we also use the first two polyphase waveforms of the polyphase code set with length 40 in [13]. The two polyphase waveforms are applied in the two transmitters, respectively. After pulse compression with matched filtering and pulse coherent integration, the range reconstruction results are shown in Figs. 8–9 with red square marks that are denoted as “MIMO P-Code.” For a better display, in this and following simulations, the pulse compression and integration gains of all the range reconstruction results are normalized.

In Fig. 8, we plot the range reconstruction results of all the transmitter and receiver pairs with $\sigma_d^2 = 1$ and without noise. Comparing with the real target amplitudes (with blue solid line with asterisk marks), the results show that the MIMO OFDM range reconstruction is precise for all the transmitter and receiver pairs. It also indicates that there is no interference between different transmitters and the full spatial diversity can be achieved by using our

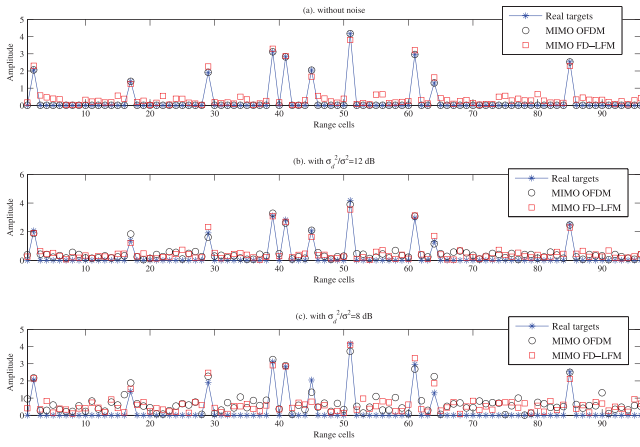


Fig. 10. Amplitudes of targets for $(\alpha, \beta) = (1, 1)$ after range reconstructions using frequency division LFM waveforms and our designed OFDM pulses. (a) Without noise. (b) With $\frac{\sigma_d^2}{\sigma_s^2} = 12$ dB. (c) With $\frac{\sigma_d^2}{\sigma_s^2} = 8$ dB.

proposed MIMO OFDM radar. Meanwhile, the benefit of the IRCI free range reconstruction by using CP-based OFDM radar still holds. However, because of the nonzero cross correlation (or nonorthogonality) between the two polyphase waveforms as well as the range sidelobes of the autocorrelation functions, some targets cannot be reconstructed correctly as shown in Fig. 8, and thus, the spatial diversity cannot be clearly obtained by using the polyphase waveforms. Moreover, the range reconstruction results of some range cells without target by using the polyphase waveforms are much larger than 0. We also consider the range reconstruction performances for $\frac{\sigma_d^2}{\sigma_s^2} = 12$ dB and 8 dB. Notice that, according to (34) and the normalized transmitted energy constraint, the SNRs of the received signals are about -10.04 dB and -14.04 dB for $\frac{\sigma_d^2}{\sigma_s^2} = 12$ dB and 8 dB, respectively. The simulation results for the transmitter and receiver pair $(\alpha, \beta) = (1, 1)$ are plotted in Fig. 9. The results show that the performances of our proposed MIMO OFDM radar are better than that by using the polyphase waveforms, especially for a larger SNR, for example, when $\frac{\sigma_d^2}{\sigma_s^2} = 12$ dB.

For further comparison, we also consider the frequency division MIMO radar, in which each transmitted waveform is assigned an independent and nonoverlapped frequency band with bandwidth B . Thus, the orthogonality of the transmitted waveforms is guaranteed in this radar system despite time delays, but \mathbb{T} times more bandwidth (i.e., $\mathbb{T}B$) is required. By using LFM waveforms and the above simulation parameters, we obtain and plot the range reconstruction results in Fig. 10 with red square marks that are denoted as ‘‘MIMO FD-LFM.’’ By comparing with the true target amplitudes, the results indicate that the performances of our proposed MIMO OFDM radar are obviously better than the MIMO FD-LFM radar for the cases without noise and $\frac{\sigma_d^2}{\sigma_s^2} = 12$ dB. It is because the IRCI across the range cells occurs by using LFM waveforms, even through the cross correlation

can be completely avoided by using frequency division. The performances of MIMO OFDM and MIMO FD-LFM are similar to each other for $\frac{\sigma_d^2}{\sigma_s^2} = 8$ dB. However, in MIMO FD-LFM the bandwidth requirement is 300 MHz, twice more. We believe that the IRCI will be more serious by using LFM waveforms when more range cells are included in targets, and the benefit of our proposed MIMO OFDM radar will be more obvious.

VI. CONCLUSION

In this paper, we proposed a novel frequency-band shared and sufficient CP-based MIMO OFDM radar range reconstruction method by using our newly proposed and designed OFDM pulses that are in the same frequency band but orthogonal to each other for every subcarrier in the discrete frequency domain. This range reconstruction algorithm with the orthogonality of the MIMO OFDM signals can provide the advantage of avoiding the interference between different transmitters, even when there are time delays among the signals from different transmitters, and achieving the full spatial diversity. Meanwhile, due to the sufficient CP insertion to each pulse with the zero head and tail values in the discrete time domain, the range reconstruction is IRCI free and the proposed system does not have the energy redundancy. Our proposed range reconstruction is a joint pulse compression and pulse coherent integration, after which the SNR was analyzed. We then proposed four design criteria for multiple OFDM pulses. To achieve the orthogonality for every subcarrier in the discrete frequency domain across multiple transmitters, COD were adopted, with which only non-zero-valued OFDM pulses for the first transmitter are needed to be designed. To maximize the SNR, a closed-form solution was proposed by using the paraunitary filterbank theory. Considering the trade-off between the PAPR and the SNR degradation within the range reconstruction, we also proposed an MICF joint OFDM pulse design method to obtain OFDM pulses with low PAPRs and insignificant SNR degradation. We finally presented some simulations to demonstrate the performance of the proposed OFDM pulse design method. By comparing with the frequency-band shared MIMO radar using polyphase code waveforms and frequency division MIMO radar using LFM waveforms, we provided some simulations to illustrate the advantage, such as the full spatial diversity and free IRCI, after the range reconstruction, of the proposed MIMO OFDM radar.

This paper provides a framework on frequency-band shared statistical MIMO OFDM radar with IRCI free and inter-transmitter-interference (ITI) free range reconstruction. Some interesting research problems remain. One of them is how to deal with the trade-off between the nonzero pulse number P_1 and the total pulse number P in a CPI. The other one would be on how to search the parameters in the paraunitary matrix to satisfy the ideal flat spectral power criterion 3) and also have good PAPR property, i.e., satisfy criterion 4).

As a final remark, this paper only considers statistical MIMO radar where multiple OFDM pulses with sufficient CP are transmitted by each transmitter in a CPI. Colocated MIMO OFDM radar has been recently considered in [36] where only one OFDM pulse with sufficient CP is transmitted in a CPI at each transmitter.

REFERENCES

- [1] Tse, D., and Viswanath, P. *Fundamentals of Wireless Communication*. New York: Cambridge University Press, 2005.
- [2] Biglieri, E., Calderbank, R., Constantinides, A., Goldsmith, A., Paulraj, A., and Poor, H. V. *MIMO Wireless Communications*. New York: Cambridge University Press, 2007.
- [3] Haimovich, A., Blum, R., and Cimini, L. MIMO radar with widely separated antennas. *IEEE Signal Processing Magazine*, **25**, 1 (2008), 116–129.
- [4] Li, J., and Stoica, P. MIMO radar with colocated antennas. *IEEE Signal Processing Magazine*, **24**, 5 (2007), 106–114.
- [5] Li, J., and Stoica, P. *MIMO Radar Signal Processing*. New York: Wiley Online Library, 2008.
- [6] Kim, J.-H., Younis, M., Moreira, A., and Wiesbeck, W. A novel OFDM chirp waveform scheme for use of multiple transmitters in SAR. *IEEE Geoscience and Remote Sensing Letters*, **10**, 3 (2013), 568–572.
- [7] Wu, X., Kishk, A., and Glisson, A. MIMO-OFDM radar for direction estimation. *IET Radar, Sonar Navigation*, **4**, 1 (2010), 28–36.
- [8] Sit, Y., Sturm, C., Baier, J., and Zwick, T. Direction of arrival estimation using the MUSIC algorithm for a MIMO OFDM radar. In *2012 IEEE Radar Conference (RADAR)*, Atlanta, GA, May 2012, pp. 0226–0229.
- [9] Sen, S., and Nehorai, A. OFDM MIMO radar with mutual-information waveform design for low-grazing angle tracking. *IEEE Transactions on Signal Processing*, **58**, 6 (2010), 3152–3162.
- [10] San Antonio, G., Fuhrmann, D., and Robey, F. MIMO radar ambiguity functions. *IEEE Journal of Selected Topics in Signal Processing*, **1**, 1 (2007), 167–177.
- [11] Somaini, U. Binary sequences with good autocorrelation and cross correlation properties. *IEEE Transactions on Aerospace and Electronic Systems*, **AES-11**, 6 (1975), 1226–1231.
- [12] Deng, H. Synthesis of binary sequences with good autocorrelation and crosscorrelation properties by simulated annealing. *IEEE Transactions on Aerospace and Electronic Systems*, **32**, 1 (1996), 98–107.
- [13] Deng, H. Polyphase code design for orthogonal netted radar systems. *IEEE Transactions on Signal Processing*, **52**, 11 (2004), 3126–3135.
- [14] Khan, H., Zhang, Y., Ji, C., Stevens, C., Edwards, D., and O'Brien, D. Optimizing polyphase sequences for orthogonal netted radar. *IEEE Signal Processing Letters*, **13**, 10 (2006), 589–592.
- [15] He, H., Stoica, P., and Li, J. Designing unimodular sequence sets with good correlations-Including an application to MIMO radar. *IEEE Transactions on Signal Processing*, **57**, 11 (2009), 4391–4405.
- [16] Song, X., Zhou, S., and Willett, P. Reducing the waveform cross correlation of MIMO radar with space-time coding. *IEEE Transactions on Signal Processing*, **58**, 8 (2010), 4213–4224.
- [17] Xu, L., and Liang, Q. Zero correlation zone sequence pair sets for MIMO radar. *IEEE Transactions on Aerospace and Electronic Systems*, **48**, 3 (2012), 2100–2113.
- [18] Jin, Y., Wang, H., Jiang, W., and Zhuang, Z. Complementary-based chaotic phase-coded waveforms design for MIMO radar. *IET Radar, Sonar Navigation*, **7**, 4 (2013), 371–382.
- [19] Zhang, T., and Xia, X.-G. OFDM synthetic aperture radar imaging with sufficient cyclic prefix. *IEEE Transactions on Geoscience and Remote Sensing*, **53**, 1 (2015), 394–404.
- [20] Zhang, T., Xia, X.-G., and Kong, L. IRCI free range reconstruction for SAR imaging with arbitrary length OFDM pulse. *IEEE Transactions on Signal Processing*, **62**, 18 (2014), 4748–4759.
- [21] Alamouti, S. A simple transmit diversity technique for wireless communications. *IEEE Journal on Selected Areas in Communications*, **16**, 8 (1998), 1451–1458.
- [22] Tarokh, V., Jafarkhani, H., and Calderbank, A. Space-time block codes from orthogonal designs. *IEEE Transactions on Information Theory*, **45**, 5 (1999), 1456–1467.
- [23] Su, W., and Xia, X.-G. On space-time block codes from complex orthogonal designs. *Wireless Personal Communications*, **25**, 1 (2003), 1–26.
- [24] Liang, X.-B., and Xia, X.-G. On the nonexistence of rate-one generalized complex orthogonal designs. *IEEE Transactions on Information Theory*, **49**, 11 (2003), 2984–2988.
- [25] Wang, H., and Xia, X.-G. Upper bounds of rates of complex orthogonal space-time block codes. *IEEE Transactions on Information Theory*, **49**, 10 (2003), 2788–2796.
- [26] Liang, X.-B. Orthogonal designs with maximal rates. *IEEE Transactions on Information Theory*, **49**, 10 (2003), 2468–2503.
- [27] Su, W., Xia, X.-G., and Liu, K. A systematic design of high-rate complex orthogonal space-time block codes. *IEEE Communications Letters*, **8**, 6 (2004), 380–382.
- [28] Lu, K., Fu, S., and Xia, X.-G. Closed-form designs of complex orthogonal space-time block codes of rates $(k + 1)/(2k)$ for $2k-1$ or $2k$ transmit antennas. *IEEE Transactions on Information Theory*, **51**, 12 (2005), 4340–4347.
- [29] Vaidyanathan, P. P. *Multirate Systems and Filter Banks*. Englewood Cliffs, NJ: Prentice-Hall, 1993.
- [30] Xia, X.-G. Multirate filterbanks. In *Wiley Encyclopedia of Electrical and Electronics Engineering*, vol. 14, J. G. Webster, Ed. New York: Wiley, 1999, pp. 35–51.

- [31] Skolnik, M. I. *Introduction to Radar Systems*. New York: McGraw-Hill, 2001.
- [32] Prasad, R. *OFDM for Wireless Communications Systems*. Boston: Artech House, 2004.
- [33] Fishler, E., Haimovich, A., Blum, R., Cimini, L., Chizhik, D., and Valenzuela, R. Spatial diversity in radars—models and detection performance. *IEEE Transactions on Signal Processing*, **54**, 3 (2006), 823–838.
- [34] Armstrong, J. Peak-to-average power reduction for OFDM by repeated clipping and frequency domain filtering. *Electronics Letters*, **38**, 5 (2002), 246–247.
- [35] Han, S. H., and Lee, J. H. An overview of peak-to-average power ratio reduction techniques for multicarrier transmission. *IEEE Wireless Communications*, **12**, 2 (2005), 56–65.
- [36] Cao, Y.-H., Xia, X.-G., and Wang, S.-H. IRCI free co-located MIMO radar based on sufficient cyclic prefix OFDM waveforms. *IEEE Transactions on Aerospace and Electronic Systems*, to be published (2015).

Xiang-Gen Xia (M'97—S'00—F'09) received his B.S. degree in mathematics from Nanjing Normal University, Nanjing, China, and his M.S. degree in mathematics from Nankai University, Tianjin, China, and his Ph.D. degree in electrical engineering from the University of Southern California, Los Angeles, in 1983, 1986, and 1992, respectively.

He was a Senior/Research Staff Member at Hughes Research Laboratories, Malibu, CA, during 1995-1996. In September 1996, he joined the Department of Electrical and Computer Engineering, University of Delaware, Newark, where he is the Charles Black Evans Professor. His current research interests include space-time coding, MIMO and OFDM systems, digital signal processing, and synthetic aperture radar (SAR) and inverse synthetic aperture radar (ISAR) imaging.

Dr. Xia has over 300 refereed journal articles published and accepted, is the holder of seven U.S. patents, and is the author of the book, *Modulated Coding for Intersymbol Interference Channels* (Marcel Dekker, 2000). He received the National Science Foundation (NSF) Faculty Early Career Development (CAREER) Program Award in 1997, the Office of Naval Research (ONR) Young Investigator Award in 1998, and the Outstanding Overseas Young Investigator Award from the National Nature Science Foundation of China in 2001. He also received the Outstanding Junior Faculty Award of the Engineering School of the University of Delaware in 2001. He is currently serving and has served as an Associate Editor for numerous international journals including *IEEE Transactions on Signal Processing*, *IEEE Transactions on Wireless Communications*, *IEEE Transactions on Mobile Computing*, and *IEEE Transactions on Vehicular Technology*. He was Technical Program Chair of the Signal Processing Symposium, Globecom 2007 in Washington, D. C., and the General Co-Chair of International Conference on Acoustics, Speech and Signal Processing (ICASSP) 2005 in Philadelphia, PA.



Tianxian Zhang received his B.S. degree from the University of Electronic Science and Technology of China (UESTC) in 2009. He is now working toward his Ph.D. degree on signal and information processing at UESTC.

From October 2012 to October 2014, he was a visiting student researcher at the University of Delaware. His current research interests include radar and statistical signal processing, and synthetic aperture radar (SAR) systems.



Lingjiang Kong was born in 1974. He received the B.S., M.S., and Ph.D. degrees from the University of Electronic Science and Technology of China (UESTC) in 1997, 2000, and 2003, respectively.

From September 2009 to March 2010, he was a visiting researcher with the University of Florida. He is currently a professor with the School of Electronic Engineering, University of Electronic Science and Technology of China (UESTC). His research interests include multiple-input multiple-output (MIMO) radar, through the wall radar, and statistical signal processing.